HYDROGEN PEROXIDE AND GLUCOSE SENSING USING MAGNESIUM FERRITE NANOPARTICLES AS PEROXIDASE MIMICS

Thesis

Submitted to the Punjab Agricultural University
in partial fulfillment of the requirements
for the degree of

INTEGRATED MASTER OF SCIENCE (HONS.)
in
CHEMISTRY
(Minor Subject: Biochemistry)

By

Ekjot Singh
(L-2015-BS-46-IM)

Department of Chemistry
College of Basic Sciences and Humanities

©PUNJAB AGRICULTURAL UNIVERSITY
LUDHIANA-141 004

2020

CERTIFICATE I

This is to certify that the thesis entitled **“Hydrogen peroxide and glucose sensing using magnesium ferrite nanoparticles as peroxidase mimics”** submitted for the degree of **5-year Integrated M.Sc. (Hons.) Programme**, in the subject of **Chemistry** (Minor subject: **Biochemistry**) of the Punjab Agricultural University, Ludhiana, is a bonafide research work carried out by **Ekjot Singh** (**L-2015-BS-46-IM**) under my supervision and that no part of this thesis has been submitted for any other degree.

The assistance and help received during the course of investigation have been fully acknowledged.

Dr. (Mrs.) Manpreet Kaur
Major Advisor
Assistant Professor
Department of Chemistry
Punjab Agricultural University,
Ludhiana-141 004, India

CERTIFICATE II

This is to certify that the thesis entitled, **“Hydrogen peroxide and glucose sensing using magnesium ferrite nanoparticles as peroxidase mimics”** submitted by **Ekjot Singh** (**L-2015-BS-46-IM**) to the Punjab Agricultural University, Ludhiana, in partial fulfillment of the requirements for the degree of **5-year Integrated M.Sc. (Hons.) Programme**, in the subject of **Chemistry** (Minor subject: **Biochemistry**) has been approved by the Student’s Advisory Committee along with External Examiner after an oral examination on the same.

(Dr. (Mrs.) Manpreet Kaur)
Major Advisor

(Dr. Hardeep Anand)
External Examiner
Associate Professor
Department of Chemistry
Kurukshetra University,
Kurukshetra, Haryana 136 119

(Dr. (Mrs.) Sucheta Sharma)
Head of the Department

(Dr. (Mrs.) G.K. Sangha)
Dean Postgraduate Studies

ACKNOWLEDGEMENT

I, ***Ekjot singh****, indepted to Almighty God, the supreme power, with whose blessings, grace and kindness, I have been able to complete a very important chapter of my life.*

I express my deep sense of gratitude and respect to my esteemed Major Advisor ***Dr. (Mrs.) Manpreet Kaur,*** *Assistant Professor, Department of Chemistry, for her inspired guidance, valuable suggestions, constructive criticism and for helping me not to give up into the struggling time during the years of study. Her innovative ideas and scientific temper inspired me a lot. Her association and untiring efforts helped me in completing the degree programme and this study in time.*

My profound respect and sincere thanks are extended to members of my Advisory committee viz. ***Dr. (Mrs.) Divya Utreja,*** *Chemist, Department of Chemistry,* ***Dr.(Mrs.) Sucheta Sharma,*** *Professor cum head, Department of Biochemistry,* ***Dr. (Mrs.) Pervinder Kaur*** *(Dean PGS Nominee), Chemist (Residue), Department of Agronomy, for their valuable suggestions and critical examination of my thesis.*

Something inexpressible, deep in my heart, the blessings of my respected parents ***S. Ranjit Singh*** *and* ***Mrs. Parveen Saini****.*

I extent my heartfelt thanks to my friend and labmate ***Komal.*** *I owe sincere thanks to* ***Jaspreet di, Manmeet di and Manpreet di*** *for their help whenever needed. My boundless emotions found no words to express their gratitude to my beloved friends* ***Kanwarpreet, Gurinder, Bikramjeet, Lovepreet, Manjot, Ravneet*** *and* ***Manminder*** *for their constant moral support, effusive encouragement, firm decisions, realistic thoughts and always a source of inspiration to me throughout my studies.*

I also owe the invaluable help rendered by lab attendants ***Bhinder aunty*** *and* ***Raj Bhaji*** *during my research work is fully acknowledged.*

Everybody may not have got mentioned, but none is forgotten. Thanks everybody. I will ever remain indebted to the many hands and good hearts that have helped me to walk on the right track. I feel proud to be a part of PAU where I spent some unforgettable moments of my life.

(Ekjot Singh*)*

Title of the Dissertation : Hydrogen peroxide and glucose sensing using Magnesium ferrite nanoparticles as peroxidase mimics

Name of the Student and Admission No. : Ekjot Singh
(L-2015-BS-46-IM)

Major Subject : Chemistry

Minor Subject : Biochemistry

Name and Designation of Major Advisor : Dr. (Mrs.) Manpreet Kaur
Assistant Professor

Degree to be Awarded : Integrated M.Sc. (Hons.) in Chemistry

Year of award of Degree : 2020

Total Pages in Dissertation : 59 + VITA

Name of University : Punjab Agricultural University, Ludhiana – 141 004
Punjab, India

ABSTRACT

Natural enzymes have been used in the food industry, biosensing and pharmaceuticals because of their high catalytic activity. However, they have some inherent drawbacks as their catalytic activity is affected by environmental conditions such as pH, temperature and inhibitors which lead to their denaturation and thus increasing operation cost. Study pertaining to materials showing properties similar to enzymes is a thrust area of research. Magnesium ferrite ($MgFe_2O_4$) NPs have gained focus of researchers because of their good catalytic activity, stability and magnetic properties. Enhanced catalytic activity can be obtained by surface coating by suitable surfactant. In this work, CTAB (cetyl trimethyl ammonium bromide) coated $MgFe_2O_4$ NPs were prepared. $MgFe_2O_4$ NPs were synthesized using sol-gel methodology and CTAB@$MgFe_2O_4$ by sonicating the CTAB with NPs in different w/w ratios. The XRD pattern of $MgFe_2O_4$ NPs confirmed single-phase formation of spinel structure with cubic symmetry. FT-IR studies confirmed presence of CTAB. Surface area, Particle size and magnetic character of the NPs were evaluated by BET, TEM and VSM respectively. CTAB@$MgFe_2O_4$ (1:1) showed best peroxidase like activity towards o-dianisidne dihydrochloride and was affected by solution pH, temperature and substrate concentration. Under optimal conditions, the as synthesized CTAB@$MgFe_2O_4$ (1:1) based system could be used for colorimetric detection of H_2O_2 in the linear range of 20-300 µM with a detection limit of 10 µM. Moreover, this system could also be used for the detection for glucose in the range of 10-1000 µM with a detection limit of 5 µM.

Keywords: Nanoparticles, Enzymes, Peroxidase

Signature of Major Advisor

Signature of the Student

ਖੋਜ ਦਾ ਸਿਰਲੇਖ : ਮੈਗਨੀਸ਼ੀਅਮ ਫੇਰਾਈਟ ਨੈਨੋਪਾਰਟੀਕਲ ਦੀ ਵਰਤੋਂ ਕਰਦਿਆਂ ਹਾਈਡ੍ਰੋਜਨ ਪਰਆਕਸਾਈਡ ਅਤੇ ਗਲੂਕੋਜ਼ ਦੀ ਸੰਵੇਦਨਾ

ਵਿਦਿਆਰਥੀ ਦਾ ਨਾਮ ਅਤੇ ਦਾਖਲਾ ਨੰ. : ਏਕਜੋਤ ਸਿੰਘ
(ਐਲ-2015-ਬੀ.ਐਸ.-46-ਆਈ.ਐਮ.)

ਪ੍ਰਮੁੱਖ ਵਿਸ਼ਾ : ਰਸਾਇਣ ਵਿਗਿਆਨ

ਸਹਿਯੋਗੀ ਵਿਸ਼ਾ : ਜੀਵ ਰਸਾਇਣ

ਮੁੱਖ ਸਲਾਹਕਾਰ ਦਾ ਨਾਮ ਅਤੇ ਅਹੁਦਾ : ਡਾ. ਮਨਪ੍ਰੀਤ ਕੌਰ
ਸਹਾਇਕ ਪ੍ਰੋਫੈਸਰ

ਡਿਗਰੀ : ਇੰਟੈਗਰੇਟਿਡ ਮਾਸਟਰ ਆਫ਼ ਸਾਇੰਸ (ਔਨਰਸ) ਜੈਵਿਕ-ਰਸਾਇਣ ਵਿਗਿਆਨ

ਡਿਗਰੀ ਨਾਲ ਸਨਮਾਨਿਤ ਕਰਨ ਦਾ ਸਾਲ : 2020

ਖੋਜ ਪੱਤਰ ਵਿੱਚ ਕੁੱਲ ਪੰਨੇ : 59 + ਵੀਟਾ

ਯੂਨੀਵਰਸਿਟੀ ਦਾ ਨਾਮ : ਪੰਜਾਬ ਖੇਤੀਬਾੜੀ ਯੂਨੀਵਰਸਿਟੀ, ਲੁਧਿਆਣਾ-141 004
ਪੰਜਾਬ, ਭਾਰਤ।

ਸਾਰ-ਅੰਸ਼

ਕੁਦਰਤੀ ਪਾਚਕਾਂ ਦੀ ਵਰਤੋਂ ਖੁਰਾਕ ਉਦਯੋਗ, ਬਾਇਓਸੈਨਸਿੰਗ ਅਤੇ ਫਾਰਮਾਸਿਟੀਕਲ ਵਿਚ ਕੀਤੀ ਗਈ ਹੈ ਕਿਉਂਕਿ ਉੱਚ ਉਤਪ੍ਰੇਰਕ ਗਤੀਵਿਧੀ ਹੈ। ਹਾਲਾਂਕਿ, ਉਨ੍ਹਾਂ ਵਿਚ ਕੁਝ ਕਮੀਆਂ ਹਨ ਜਿਵੇਂ ਕਿ ਉਨ੍ਹਾਂ ਦੀ ਉਤਪ੍ਰੇਰਕ ਗਤੀਵਿਧੀਆਂ ਵਾਤਾਵਰਣ ਦੀਆਂ ਸਥਿਤੀਆਂ ਜਿਵੇਂ ਪੀਐਚ, ਤਾਪਮਾਨ ਅਤੇ ਰੋਕਣ ਵਾਲੇ ਅਣੂਆਂ ਦੁਆਰਾ ਪ੍ਰਭਾਵਿਤ ਹੁੰਦੀਆਂ ਹਨ ਜਿਹੜੀਆਂ ਉਨ੍ਹਾਂ ਦੇ ਨਿਘਾਰ ਦਾ ਕਾਰਨ ਬਣਦੀਆਂ ਹਨ ਅਤੇ ਇਸ ਤਰ੍ਹਾਂ ਕੰਮ ਦੀ ਲਾਗਤ ਵਿੱਚ ਵਾਧਾ ਹੁੰਦਾ ਹੈ। ਮੈਗਨੀਸ਼ੀਅਮ ਫੈਰਾਈਟ ਨੇ ਖੋਜਕਰਤਾਵਾਂ ਦਾ ਧਿਆਨ ਉਨ੍ਹਾਂ ਦੀ ਚੰਗੀ ਉਤਪ੍ਰੇਰਕ ਗਤੀਵਿਧੀ, ਸਥਿਰਤਾ ਅਤੇ ਚੁੰਬਕੀ ਵਿਸ਼ੇਸ਼ਤਾਵਾਂ ਦੇ ਕਾਰਨ ਪ੍ਰਾਪਤ ਕੀਤਾ ਹੈ। ਵਧੀ ਹੋਈ ਉਤਪ੍ਰੇਰਕ ਕਿਰਿਆ ਨੂੰ ਸਰਫੈਕਟੈਂਟ ਦੁਆਰਾ ਸਤਹ ਕੋਟਿੰਗ ਦੁਆਰਾ ਪ੍ਰਾਪਤ ਕੀਤਾ ਜਾ ਸਕਦਾ ਹੈ। ਇਸ ਕੰਮ ਵਿੱਚ ਸੀਟੀਲ ਟ੍ਰਾਈਮੇਥੀਲ ਅਮੋਨੀਅਮ ਬਰੋਮਾਈਡ ਕੋਟੇਡ ਫੈਰਾਈਟ ਤਿਆਰ ਕੀਤਾ ਗਿਆ ਸੀ। ਫੈਰਾਈਟ ਨੂੰ ਸੋਲ-ਜੈੱਲ ਵਿਧੀ ਅਤੇ ਸੀਟੀਏਬੀ @ ਫੈਰਾਈਟ ਨੂੰ ਵੱਖੋ ਵੱਖਰੇ ਭਾਰ / ਭਾਰ ਅਨੁਪਾਤ ਵਿਚ ਸੀਟੀਏਬੀ ਨਾਲ ਸੋਨੀਕੇਟ ਕਰਕੇ ਸੰਸਲੇਸ਼ਣ ਕੀਤਾ ਗਿਆ ਸੀ। ਫੈਰਾਈਟ ਨੈਨੋ ਕਣਾ ਦੇ ਐਕਸ ਰੇ ਨੇ ਘਣ ਪ੍ਰਣਾਲੀ ਨਾਲ ਸਪਿਨਲ ਬਣਤਰਾਂ ਦੇ ਇੱਕੋ ਦੇ ਗਠਨ ਦੀ ਪੁਸ਼ਟੀ ਕੀਤੀ। ਨੈਨੋ ਕਣਾ ਦਾ ਆਕਾਰ ਅਤੇ ਜਾਲੀ ਨਿਰੰਤਰ ਐਕਸ ਰੇ ਡਾਟਾ ਦੀ ਵਰਤੋਂ ਨਾਲ ਪ੍ਰਾਪਤ ਕੀਤੇ ਜਾਂਦੇ ਹਨ। FT-IR ਅਧਿਐਨ ਨੇ ਸੀਟੀਏਬੀ ਦੀ ਮੌਜੂਦਗੀ ਦੀ ਪੁਸ਼ਟੀ ਕੀਤੀ। ਸਤਹ ਖੇਤਰ, ਕਣ ਦਾ ਆਕਾਰ ਅਤੇ ਐਨ ਪੀ ਦੇ ਚੁੰਬਕੀ ਚਰਿੱਤਰ ਦਾ ਕ੍ਰਮਵਾਰ BET, TEM ਅਤੇ VSM ਦੁਆਰਾ ਮੁਲਾਂਕਣ ਕੀਤਾ ਗਿਆ। ਸੀਟੀਏਬੀ ਵਾਲੇ ਮੈਗਨੀਸ਼ੀਅਮ ਫੈਰਾਈਟ (1: 1) ਨੇ ਓ-ਡਾਇਨਿਸਡਿਨ ਡੀਹਾਈਡ੍ਰੋਕਲੋਰਾਈਡ ਪ੍ਰਤੀ ਸਰਗਰਮੀ ਜਿਹੀ ਸਰਬੋਤਮ ਪਰਆਕਸਾਈਡਸ ਦਰਸਾਈ ਅਤੇ ਘੋਲ ਪੀਐਚ, ਤਾਪਮਾਨ ਅਤੇ ਘਟਾਓਣਾ ਡੋਜ਼ ਤੋਂ ਪ੍ਰਭਾਵਤ ਹੋਇਆ। ਅਨੁਕੂਲ ਸਥਿਤੀਆਂ ਦੇ ਤਹਿਤ, ਅਧਾਰਤ ਸਿਸਟਮ ਨੂੰ 10 ਮਾਈਕਰੋ ਮੋਲ ਦੀ ਖੋਜ ਸੀਮਾ ਦੇ ਨਾਲ 20-300 ਮਾਈਕਰੋ ਮੋਲ ਦੀ ਰੇਖੀ ਰੇਂਜ ਵਿੱਚ H_2O_2 ਦੀ ਮਾਤਰਾ ਜਾਨਣ ਲਈ ਵਰਤਿਆ ਜਾ ਸਕਦਾ ਹੈ। ਇਸ ਤੋਂ ਇਲਾਵਾ, ਇਹ ਪ੍ਰਣਾਲੀ 10-1000 ਮਾਈਕਰੋ ਮੋਲ ਦੀ ਸੀਮਾ ਵਿੱਚ ਗਲੂਕੋਜ਼ ਦੀ ਖੋਜ ਲਈ 5 ਮਾਰੀਕਰੋ ਮੋਲ ਦੀ ਖੋਜ ਸੀਮਾ ਦੇ ਨਾਲ ਵੀ ਵਰਤੀ ਜਾ ਸਕਦੀ ਹੈ।

ਮੁੱਖ ਸ਼ਬਦ: ਨੈਨੋਪਾਰਟੀਕਲਸ, ਇੰਜ਼ਾਈਮਸ, ਪਰਆਕਸਦੀਡੇਜ਼

ਪ੍ਰਮੁੱਖ ਸਲਾਹਕਾਰ ਦੇ ਹਸਤਾਖਰ

ਵਿਦਿਆਰਥੀ ਦੇ ਹਸਤਾਖਰ

CONTENTS

CHAPTER I

INTRODUCTION

The term “artificial enzyme” is used for an enzyme prepared synthetically that performs the same function as the native ones. Enzymes are the biological catalyst which enhances the rate of reaction. Enzymes are substrate specific and possess higher catalytic efficiency therefore widely used in agro industries, chemical industries and in food processing units. But they are susceptible to change in temperature and pH which leads to their denaturation. To overcome these drawbacks artificial enzymes have gained great interest (Daniel *et al* 1996). Nanoparticles (NPs) are submicron particles ranging from 1-100 nm. As size of the material is decreased its properties change because its surface to volume ratio changes. Sometimes on changing the size different properties like optical, electrical and magnetic gets altered which are not shown by the bulk material. Thus, they show interesting biological and physio-chemical applications (Batista *et al* 2015).The term “‘nanozymes” was initially coined by Pasquato *et al* (2015). Nanozymes have already found wide applications in diverse fields including biosensors, pharmaceutical processes, and the food industry. To date, a wide range of nanozymes have been identified including metal NPs (Long *et al* 2011), metal oxide NPs (Natalio *et al* 2012) and carbon-based nanostructures (Shi *et al* 2011). Peroxidase, oxidase, superoxide dismutases (SOD) and catalase mimic activity by nanozymes is of great interest (He *et al* 2015). Different forms of nanozymes are reported such as rods, fibers, wires, tubes, and ribbons (Narita 2019), nanopopcorns (Wu *et al* 2019). They have intrinsic property to act as enzyme mimic (Wang *et al* 2019).

Hydrogen peroxide is present in nature as well as in biological systems. Sea water has 0.5 to 14 μg/L, freshwater has 1 to 30 μg/L and air 0.1 to 1 part per billion of hydrogen peroxide (Offermanns *et al* 2000). Hydrogen peroxide is a mild antiseptic used on the skin to avoid infection of minor cuts, scrapes, and burns. It may be used as a mouth rinse to help remove mucus or to relieve minor mouth irritation. Hydrogen peroxide is used to whiten the teeth; it oxidizes the organic matrix to enhance whiteness. However, undue use of hydrogen peroxide can cause damage to the human body, including neurodegenerative disorders, duodenal lesions and diabetes (Valko *et al* 2007). Detection of hydrogen peroxide is carried by colorimetric, electrochemical, chemiluminscence and fluorescent methods. As compared to other methods, colorimetric method does not require sophisticated instrumentation or pre treatment and is also cost effective. It also has the advantage that results are interpreted with naked eye i.e. Visual detection. Chromogenic substrate like o-dianisidine dihydrochloride, tetrahydrobioprotein, 3,3’,5,5’-Tetramethylbenzidine are used which can reduce the hydrogen peroxide with the help of artificial enzyme (Yang *et al* 2016).

Glucose is an important source of vitality for cell action in the humans. It is essential to keep up an appropriate level of glucose in the blood, and the homeostatic framework in human physiology (e.g., endocrine and the nervous system) firmly manages the glucose level. However, a few patients experience the ill effects of metabolic issue including glucose processing, which results in the injurious outcomes (Petersen *et al* 2017). Diabetes mellitus is the most pervasive infection identified with these outcomes, and it is a standout amongst the most far reaching constant illnesses coming about because of the dysfunction of the insulin secretion. Excess levels of glucose in the blood plasma prompts a hyperglycemic condition, which causes various difficulties, for example, cardiovascular scatters, and kidney failure and vision impairment. Due to the extreme medicinal consequences of diabetes related difficulties, there is a basic requirement for individual checking and control of the blood glucose level (Taylor *et al* 2019). Thus, glucose sensors have been created to precisely estimate the blood glucose level. Among various techniques for glucose estimation, optical (Shukla *et al* 2017) and electrochemical (Zaidi and Shin 2016) examinations have been broadly explored. Optical methods utilize the change of colour in an indicator that reflects the concentration of glucose. The colour of the indicator changes during an enzymatic reaction that converts glucose to its metabolites.

Nanoparticles (NPs) can be synthesized by different routes such as sol-gel, combustion, co-precipitation methods, hydrothermal reactions (Lassoued *et al* 2018). Most useful method for synthesizing nanoferrites is combustion method because of the homogeneous particle size distribution (Kaur *et al* 2015). Superparamagnetic properties are shown by iron NPs which are synthesized by ferrites (Haikarainen *et al* 2011). It has been shown by Yang *et al* (2014) that magnetic NPs of Fe_3O_4 because of their biological and chemical properties possess similar enzymatic properties as of natural peroxidases. Ferrofluids or magnetic fluids are the aqueous suspension of NPs of iron oxide, used in bioscience and medicine. Biocompatible magnetic fluids are used in magnetic resonance imaging (Chourpa *et al* 2005).

Magnetic NPs such as ferrite NPs have gained researchers' attention due to their use in magnetic fluids, data storage (Chakradhary *et al* 2019), and bio-applications (Ashour *et al* 2018). Bio applications include detection of biological entities like enzymes, nucleic acids, bacterial proteins, and several viruses and clinical diagnosis.

Ferrites are ceramic materials made by large proportions iron (III) oxide blended with small proportions of one or more additional elements. Properties of ferrite nanoparticles are determined by chemical composition, particle size and interaction of particle with the surrounding matrix. They are widely used in electronic, magnetic and microwave devices. Ferrites possess different enzyme like activity. Verma *et al* (2019) showed the presence of superoxide dismutase like activity of MFe_2O_4 (M= Mn, Co, Cu) while cerium doped ferrite

($Ce–Fe_3O_4$ NPs) (Hosseini *et al* 2017),N-doped zinc ferrite $ZnFe_2O_4$ (Navadeepthy *et al* 2017) have peroxidase like activity and these were used in the detection of H_2O_2 and glucose (Su *et al* 2012). Magnesium ferrite ($MgFe_2O_4$) possesses catalytic and magnetic properties and is also stable in nature. MoS_2@$MgFe_2O_4$ composites were synthesized and reported to have flower like structure. These composites showed peroxidase mimicking activity. This system was used for the colorimetric determination of H_2O_2 and glucose in the range of 2.5–300 μM and 5.0–200 μM respectively with the detection limit of 2.0 μM for glucose (Zhang *et al* 2018).

Surfactants are the compounds which bring changes in the physio-chemical properties of NPs. They enhance the surface area which in turn increases the catalytic activity of nanozymes. Surfactants are of four types, these are- nonionic (sorbitan alkyl esters), anionic (Dioctyl sodium sulfosuccinate, sodium lauryl ether sulfate), cationic (cetyl trimethyl ammonium bromide and cetyl trimethylammonium chloride), amphoteric (cocamidopropyl betaine).

Thus, the role of surfactant coating on $MgFe_2O_4$ NPs as peroxidase mimics is a thrust area of research. The main objectives of this study were:

1. To synthesize $MgFe_2O_4$ NPs using the sol-gel method.
2. To synthesize the surfactant coated $MgFe_2O_4$ NPs using the ultrasonication method.
3. To study the peroxidase mimic activity of synthesized compounds
4. To detect hydrogen peroxide and glucose using CTAB@$MgFe_2O_4$ peroxidase system.

The thesis runs into four chapters, namely, review of literature, materials and methods, results and discussion, which is followed by the summary. The prepared NPs were characterized by using different physio-chemical techniques. The mechanism of enzyme mimic activity was studied. The influence of various factors affecting enzyme mimic activity such as pH, contact time, catalyst dose, temperature, and initial substrate concentration was also studied. The synthesized NPs were used for hydrogen peroxide and glucose sensing under optimized reaction conditions.

CHAPTER II

REVIEW OF LITERATURE

Nanozymes are artificial enzymes with properties such as good catalytic activity, high stability, low cost in comparison to the natural enzymes due to these applications; they act as a bridge between nanotechnology and biology. These have applications in biosensing, bioimaging to therapeutics and environmental remediation. A nanozyme can be a metal oxide (Chen *et al* 2019), metal (Li *et al* 2015), multi-metal (Pandey *et al* 2015), metal hydroxide (Chen *et al* 2013), metal sulfide (Niu *et al* 2016), metal organic framework (Zhang *et al* 2014), and ferrite (Fan *et al* 2012). All of these were extensively studied by the researchers in the last two decades except ferrites. Ferrite NPs are magnetic in nature and better than pure metal NPs because of their low cost, ease of synthesis and stable nature thus, these are widely used in magnetic, electronic and microwave devices, apart from it now they have been explored for their adsorptive and catalytic properties and have intrinsic enzyme mimic activity. The literature reviewed related to the present research is documented under following subtitles i.e. synthesis of NPs and their applications as enzyme mimics.

2.1 Synthesis of Nanoparticles

Various methods like hydrothermal, co-precipitation, sonochemical, and sol-gel have been used for the synthesis of different NPs. These NPs were characterized by different techniques including FT-IR (Fourier Transform Infrared Spectroscopy), BET (Brunauer Emmet Teller) analysis, SEM (Scanning Electron Microscopy), TEM (Transmission Electron Microscopy), XRD (X-Ray Diffraction) and VSM (Vibrating Sample Magnetometer). Till date, several methods including physical and chemical methods have been reported for synthesis of MFe_2O_4 NPs (Majidi *et al* 2016). Chemical methods are bottom up approaches while physical methods are top down approaches and are illustrated in scheme 1.

In the physical methods, laser pyrolysis technique involves excitation of a compound using laser radiation and transmittance of energy to a reaction medium occurs that elevate the temperature of the reaction medium. The reactants decompose and formation of NPs takes place (D’Amato *et al* 2013). In high energy ball milling, mixtures of metal salts are placed in the ball mill for high-energy oscillations from the balls that leads to formation of nanosized particles (Salah *et al* 2011). Electric arc deposition process involves use of high vapour pressure by electron bombardment in vacuum to heat the material and is transported by diffusion (Antisari *et al* 2003). Physical and electrical properties of target are changed in ion implantation method by setting up ions of an element into solid (Sawai *et al* 2014).

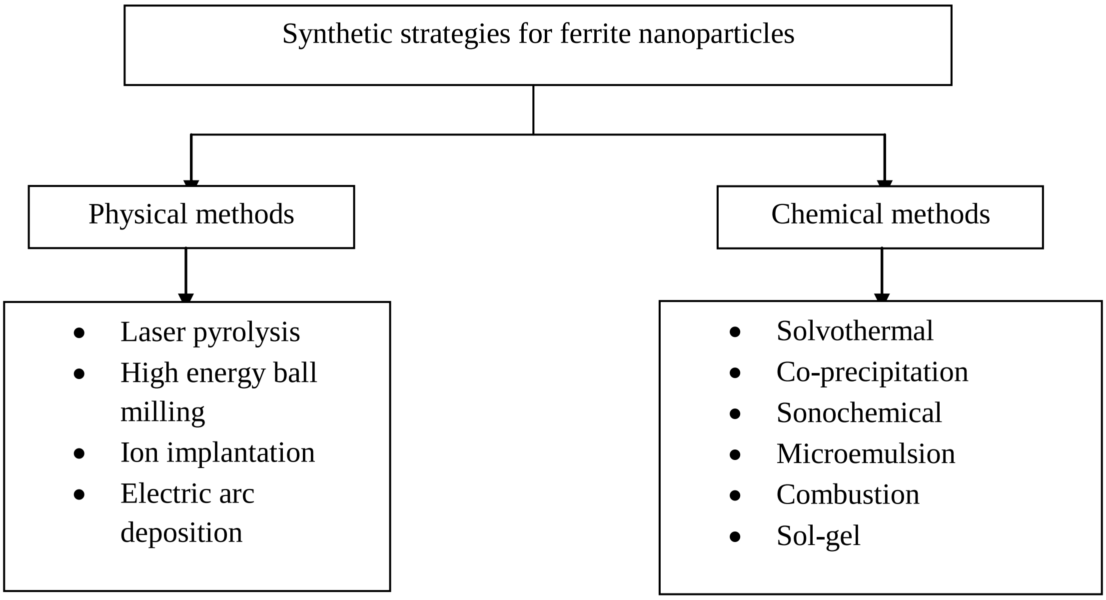

Scheme 1: Synthetic methods for synthesis of ferrite nanoparticles

Among the chemical methods, solvothermal process involves usage of solvent under moderate to high pressure (from 1 atm to 10,000 atm) and temperature ranges from 100 to 1000°C to facilitate the contact of reactants during synthesis (Komarneni and Katuski 2010). If the solvent is water then this method is named as ‘hydrothermal synthesis’. In Co-precipitation method, precipitation of metal cations as oxalates, citrates, carbonates or hydroxides takes place. The precipitates are dried and heated to the requisite temperature and final product is obtained (Kaur and Kaur 2014). Sound waves are used in sonochemical method (Nag *et al* 2012). The metal oxide particles come in contact with shock waves produced by cavitation bubbles and collide at high speed. The energy produced from this reaction leads to the formation of ferrite NPs. Microemulsion method is classified into normal micelle method and reverse micelle method. It involves the use of surfactants above the critical micelle concentration (Cao *et al* 2008). Combustion process involves exothermic reaction between a fuel and an oxidizer (Kaur and Kaur 2014). Sol-gel method includes various processes lie hydrolysis, gelation, polymerization, dehydration, drying and densification. In this method conversion of sol to gel occur thus so named (Kaur *et al* 2015).

2.1.1 Synthesis of magnesium ferrite nanoparticles ($MgFe_2O_4$ NPs)

Magnesium ferrite ($MgFe_2O_4$) NPs were successfully synthesized by electrospinning method by Maensiri *et al* (2009). X-ray diffraction, FT-IR, scanning electron microscopy, and transmission electron microscopy showed that calcination of the as-spun $MgFe_2O_4$/poly(vinyl pyrrolidone) (PVP) composite nanofibers for 2 h at 500–800°C in air resulted in spinel $MgFe_2O_4$ nanostuctures.The crystal structure and morphology of the NPs were influenced by the calcination temperature. Crystallite size of the NPs contained in nanofibers elevated from 15 to 24 nm when calcination temperature was raised from 500°C to 800°C.

$MgFe_2O_4$ NPs have also been synthesized by Chen *et al* (1999) by coprecipitation method. Magnetic measurements and neutron diffraction have determined the presence of a superparamagnetic state in this metal oxide system. Mössbauer spectroscopy had been used to study the superparamagnetic relaxation of magnetization in these NPs. The results are consistent with Néel theory. Magnesium spinel ferrite nanoparticles were prepared using co-precipitation assisted by ultrasonic irradiation method. The starting material used was ammonium ferrous sulfate and magnesium sulfate heptahydrate. These were dissolved in doubly distilled water and treated with 5 M NaOH solution to form a precipitate at pH 11. The resultant was filtered, washed and dried at 120°C. The formed powder was calcined for 2 h at 600°C using ultrasound irradiation (Rashad 2007).

Verma *et al* (2004) employed hydrothermal method for the fabrication of ferrite NP with average size of 3 nm as predicted by XRD and electron microscopy studies. VSM studies showed the presence of superparamagnetic state of the ferrite NPs. The reaction was carried out in a microwave accelerated system which operates at 2.45 GHz frequency. Magnesium nitrate, Ferric nitrate and Potassium hydroxide were used as starting chemicals for the synthesis of $MgFe_2O_4$NPs, aqueous solutions of the metal nitrates, in the stoichiometric 1:2 molar ratio. Reactions were carried out under mild conditions of 50 psi pressure and 150°C temperature and hold time of 25 minutes. After this treatment, the slurry was washed with distilled water and finally dried at 80°C in oven.

$MgFe_2O_4$ was synthesized by a convenient, environment friendly, inexpensive and efficient solid state reaction of inorganic reagents. In the beginning, $MgSO_4$, $Fe(NO_3)_3{\cdot}9H_2O$, NaOH and NaCl were mixed in the molar ratio 1:2:8:10 and placed in a mortar for 30 minutes. As the reaction proceeds mixture became mushy and underwent colour change. The mixture was annealed at 700°C for 1 h in a quartz tube and then allowed to cool at room temperature. Samples were washed with distilled water and dried in an oven to obtain $MgFe_2O_4$ NPs. (Liu *et al* 2005).

Sol-gel method involves mixing of metal nitrates with citric acid in a definite stochiometric molar proportion. Huang *et al* (2005) reported the synthesis of $MgFe_2O_4$ NPs by dissolving ferric nitrate and magnesium nitrate (0.50 M and 0.25 M respectively) in deionized water. Equimolar amount of citric acid was added and solution was stirred for several hours at 60°C. Then, it was heated to 80°C and gel was formed. Gel was heated at 200°C and then placed in muffle furnace. Similar protocol was employed by various scientists by varying concentrations of metal nitrates and other reaction conditions. Liu *et al* (2007) also fabricated $MgFe_2O_4$ NPs by sol gel method. Fe $(NO_3)_3.9H_2O$ (0.016 mol) and Mg $(NO_3)_2.6$

H_2O (0.008 mol) were dissolved in 20 mL deionized water to form a mixture. This mixture was magnetically stirred for 60°C and ammonia was added to adjust the pH of the solution. Sol transformed into black gel after 10 h of stirring. The gel was dried at 120°C and expanded about 10 times in volume. Gel was calcined for 2 h until the brown product formed. Another method was also reported by Fardood *et al* (2017) for the synthesis of $MgFe_2O_4$ NPs by sol gel method without the addition of external surfactant. Magnesim nitrate and ferric nitrate were used as starting materials. Initially, tragacanth gum (TG) was dissolved in deionized water and stirred for 70 min at 65°C to achieve a lucid solution. After that, Mg $(NO_3)_2$.6 H_2O and Fe $(NO_3)_3$.$9H_2O$ were added to the solution and container was placed in a sand bath. The temperature of the sand bath was fixed at 80°C and continuous stirring for 11 h to obtain a brown colour resin. The final product was calcined at 500°C in air to obtain the magnetic NPs.

Polymeric precursor method has been used to synthesize $MgFe_2O_4$ NPs. Citric acid was added to water under constant stirring at temperature of 60-70°C. Iron nitrate and magnesium carbonate in 3:1 molar ratio and ethylene glycol was added to the solution. Temperature was elevated to 110°C to promote esterification and a polymeric resin was obtained. The resin was given heat treatment for 1 h leading to the formation of powder precursor. Metal oxide powder was calcined at 500-1100°C at heating treatment of 10°C/min in ambient atmosphere and desired product was obtained. (Candeia *et al* 2006).

A single-step synthesis of $MgFe_2O_4$ NPs with an average size of 8.5 nm synthesized via mechano-chemical processing of oxide precursors at 25-35°C. Stochiometric ratio of Fe_2O_3 and MgO reactants were milled for 12 h in a ball mill at room temperature. Tungsten carbide made balls and grinding chamber was used. The ball to powder weight ratio was 20:1. Whole experiment was carried out in air at 600 rpm (Šepelák *et al* 2006). Pradhan *et al* (2005) placed MgO and Fe_2O_3 in grate mortar under double-distilled acetone for more than 6 h. High energy ball miling of the mixture was carried out with a planetary ball mill. Milling was done at room temperature in a cromesteel vial. Ball to powder mass ratio was 40:1. The rotation speed of the vial was 475 rpm while that of disc was 325 rpm. Time of milling was varied from 1 to 10 h. XRD analysis revealed the formation of the various products obtained at different milling time.

Ichiyanagi *et al* (2007) synthesized the ferrite NPs by wet chemical method using a mixture of magnesium chloride, ferric chloride and Na_2SiO_4.$9H_2O$. The resulting precipitates were washed many times with distilled water and then dried in a water hot water bath at 350 K. The resulting solids were annealed at temperatures between 800°C and 1000°C. All samples were quenched in air at 25°C to obtain the products.

Randhawa *et* a*l* (2016) reported thermolysis protocol for the fabrication of magnesium ferrite NPs. Thermal decomposition of magnesium hexapropionatoferrate (III) has been carried out in air at a heating rate of 10°C/min. During this process, precursor is first decomposed into ferrous oxalate (FeC_2O_4) and magnesium oxalate (MgC_2O_4) at 160°C. When heated at 400°C the mixture gets decomposed to form MgO and α-Fe_2O_3. Above 400°C both of these underwent decomposition to form magnesium ferrite. Identity of these compounds is established by calcinations in nickel crucible. Reaction temperature of this method is lower than the conventional ceramic methods. Ferrite NPs can also be prepared by a heat treatment method by using poly vinyl alcohol as a capping agent and Mg and Fe nitrates as sources of metal. Thermal treatment was given using an electric cylinder in air at temperatures between 400°C and 700°C and magnesium ferrite NPs were produced with size varying from 5 to 8 nm (Naseri *et al* 2014).

A single step synthesis reaction was put forth by Patil *et al* (2011). The precursors used were magnesium nitrate, ferric nitrate and glycine was used as fuel. The oxidizer to metal ratio was 5:3 which provides maximum exothermicity during the reaction. Metal nitrates were added with continuous stirring into the deionized water and then heated on a hot plate. After prolonged heating water vapours were removed and gel was formed. Persisted heating gives pure phase $MgFe_2O_4$ raw powder through a single step combustion reaction with liberation of voluminous gases. The raw powders of $MgFe_2O_4$ were calcined at 500°C in air to remove the carbon residue remained if any, during the combustion process.

Magnesium ferrite NPs have been fabricated by ethylene diamine tetraacetic acid (EDTA)-based sol–gel combustion method where EDTA was used as an organic precursor agent. Fixed amount of Fe $(NO_3)_3$ and MgO in the molar rario 2:1 were dissolved in nitric acid. The obtained solution was stirred at room temperature for 2 h until a transparent solution was formed using EDTA. The molar ratio of total metal cations to EDTA concentration is fixed to unity. The resultant solution was stirred for another 1 h for complete homogeneity and followed by evaporation untill a dried gel was formed. The obtained gel was dried at 250°C for one day to remove the adsorbed water and calcined at 400-600°C for 3 h in open to remove the contamination of organic compounds (Hussein *et al* 2015).

Large scale production of magnesium ferrite through an environmentally friendly molten salt route was reported by Lou *et al* (2014). Stochiometric amounts of nitrates of iron and magnesium alongwith NaCl and KCl were mixed thoroughly in mortar for 30 min. Then mixture was placed in a ceramic crucible, inserted into a quartz tube, heated at 5°C/min upto annealing temperature of 900°C for 4 h, and cooled at room temperature. The as synthesized material was washed several times with double-distilled water and dried at 100°C overnight in a drying oven.

Table 2.1: Synthesis of $MgFe_2O_4$ NPs by various methods

S. No.	Method	Reaction Period and Temp (^oC)	Reference
			$MgFe_2O_4$ NPs
1.	Solvothermal/Hydrothermal	Hours-day, 150	Verma *et al* 2004
2.	Sol-gel	Hours, 100-400	Liu *et al* 2007
3.	Co-Precipitation	Hours, 30-90	Chen *et al* 1999
4.	Combustion	Hours-day, 20-140	Nguyen *et al* 2019
5.	Ball milling	Hours, 20-30	Pradhan *et al* 2005
6.	Thermolysis	Hours, 150-450	Randhawa *et al* 2016

2.1.2 Synthesis of surfactant coated ferrite NPs

Surfactants are the compounds which bring changes in the physio-chemical properties of NPs. They enhance the surface area which in turn increases the catalytic activity of nanozymes. Surfactants are of four types, these are- nonionic (Sorbitan alkyl esters), ionic (Dioctyl sodium sulfosuccinate, Sodium lauryl ether sulfate), cationic (cetyl trimethylammonium bromide (CTAB) and cetyl trimethylammonium chloride), amphoteric (cocamidopropyl betaine). CTAB increased the surface area of of Fe_2O_3 NPs and enhanced the peroxidase activity (Garg *et al* 2018). $[NH_4Fe(SO_4)_2.6H_2O]$ and $[(NH_4)_2Fe(SO_4)_2.6H_2O]$ were dissolved in distilled water with stirring. To form precipitates, ammonium hydroxide was added to the solution dropwise with continuous stirring for 40 min with heating at 85°C. CTAB was added in w/w ratio of 1:1 and 1:2 in the reaction mixture. Precipitates formed were separated by centrifugation. Filtrate was washed with ethanol followed by distilled water any times until the pH of the filterate became 7. Filterate was dried in an oven at 100°C for 8h and desired products were obtained. Another method for the fabrication of CTAB coated NPs was reported by Yin *et al* (2015). Nickel ferrite nanoparticles coated with oleic acid was synthesized using polyol method. NPs of nickel were dispersed in the oleic acid solution and mixed using ultrasonic bath. The coverage of oleic acid solution was assured by the zeta potential measurement.

The gold nanorods were coated with CTAB by Lau *et al* (2011) using seed mediated method in aqueosus solutions. The seed solution was made by using freshly prepared, ice cold $NaBH_4$ (0.5 mL, 0.01M) into a mixture composed of CTAB (10 mL,0.1 M) and $HAuCl_4$ (0.25 mL, 0.01M). The seed solution was kept at room temperature for 3 h before its use. The growth solution was prepared by the sequential addition of $AgNO_3$ (0.5 mL), $HAuCl_4$(2 mL, 0.01 M), HCl (1 mL,1.0M) and ascorbic acid (0.32 mL, 0.1 M) into CTAB (40 mL,0.1 M). After mixing, the resultant solution by swirling for 1 min, 0.2 mL of the seed solution was injected. The solution was mixed by inversion for 3 min and left undisturbed overnight.

Magnesium ferrite NPs were coated with molybdenum disulfide ($MoS_2@MgFe_2O_4$) by a novel synthesis route.130 mg ammonium tetrathiomolybdate was dissolved in 50 mL DMF and 1 mL $N_2H_4.H_2O$ was slowly added to the solution and sonicated for 1 h. Then 50 mg as prepared $MgFe_2O_4$ was homogeneously dispersed in the mixture. Then, the mixture was transferred into a 100 mL autoclave and held at 200°C for 10 h. After cooling to room temperature, the precipitates were centrifuged, washed several times with distilled water and ethanol and then dried at 70°C overnight. To synthesize $MoS_2@MgFe_2O_4$ in different ratios, different amount of ATMM were dissolved in DMF in the first step (Zhang *et al* 2018).

2.2 Enzyme mimics activity of NPs and sensing of various metabolites

Nanozymes are the class of catalysts which mimic natural enzymes for catalyzing wide range of chemical and biological reactions.They can act as potential and viable alternative to the natural enzymes. They possess similar catalytic activities to their natural counterparts but have advantages of higher catalytic efficiencies, stability and controlled synthesis in lower cost. Different materials *e.g.* polymers, metal complexes, inorganic NPs can be used as nanozymes. Inorganic NPs offer higher stability, large surface areas as enzyme mimics when compared to natural enzymes (Ragg *et al* 2016). Su *et al* (2015) reported that $MgFe_2O_4$, $NiFe_2O_4$ and $CuFe_2O_4$ possess catalytic activity similar to those of biological enzymes such as peroxidase and catalase. These NPs not only could catalyze hydrogen peroxide (H_2O_2) to form hydroxyl radicals, which oxidized chromogenic peroxidase substrate to produce color but also carry out the decomposition of H_2O_2 into water and oxygen directy through catalase lie activity. Under ideal conditions, it was found that $NiFe_2O_4$ NPs showed the best peroxidase activity and used to detect glucose under optimum conditions. As a colorimetric sensor, glucose was detected in the range 9.4×10^{-7} to 2.5×10^{-5} mol L^{-1} with a limit of detection (LOD) of 4.5×10^{-7} mol L^{-1}. This biosensor was also used to detect glucose in urine sample successfully.

Interaction between nanoceria (CeO_2 nanoparticles) and H_2O_2 using DNA as probe resulted in the development of a fluorescent, sensitive biosensor for hydrogen peroxide. When reaction was coupled with glucose oxidase it was possible to detect glucose in the blood serum. It can detect hydrogen peroxide with the range down to 4.4 parts-per-billion (130nM) and glucose upto 8.9μM in the buffer (Liu *et al* 2015). Well redispersed CeO_2 nanoparticles were synthesized with a narrow size distribution through a low cost, simple and rapid hydrothermal method. These prepared nanoparticles were shown to have peroxidase-like catalytic activity at varied range of temperature and pH as compared to natural enzymes. These synthesized nanoparticles also have more affinity than natural enzyme towards TMB (Jiao *et al* 2012).

Gold nanodiamonds exhibit catalytic activity for the oxidation of o-phenylenediamine in the presence of hydrogen peroxide similarly to a peroxidase enzyme. ND-gold composite could be employed for analysis of biological samples in merger with natural enzyme (Kim *et al* 2016). Positively charged gold nanoparticles have intrinsic peroxidase like activity. It catalyzes oxidation of TMB (3,3,5,5-tetramethylbenzidine) to form a blue colour aqueous solution by H_2O_2. This provides a simple way for the colorimetric detection of glucose and H_2O_2(Jv *et al* 2010).

Hu *et al* (2013) reported that copper nanoclusters have internal peroxidase like activity. The increase in absorbance due to catalytic reaction by copper nanoclusters allows the detection of H_2O_2 with detection limit of 10µM in the range of 10µM-1mM. Owing to this finding a selective and simple colomertric assay for glucose detection was these nanoclusters have several advantages over natural enzymes such as low cost ease of preparation and activity under harsh conditions.

In order to investigate the peroxidase-like activity of CdS NPs, the catalytic oxidation of a peroxidase substrate as TMB has been studied in presence of H_2O_2. The reaction was monitored by following the increase of absorbance at 653 nm with time which originated from the oxidation product of TMB, similar to the phenomenon observed for the commonly used horse radish peroxidase enzyme. The CdS NPs show excellent photocatalytic degradation for organic pollutants (RB) for their probable application in waste water treatment peroxidase-like activity of them was also examined and suitable results as artificial peroxidases have been found by Maji *et al* (2012).

CoS catalyzed the oxidation of peroxidase substrate 3,3’,5,5’-tetramethylbenzidine (TMB) in the presence of H_2O_2 to produce blue colour solution, which is the principle used for H_2O_2 sensing. The linearity of H_2O_2 detection ranges from 0.05-0.8 mM. Owing to strong affinity of mercury ions towards thiol compounds, an “on-off” calorimetric sensor was developed which ranges from 0.25-3 µM (Yang *et al* 2016).α-Fe_2O_3 acts as a catalyst with catalase-like activity that can efficiently convert H_2O_2 into O_2 and it was found that nanozyme dressing significantly reduce harmful effects of H_2O_2. As H_2O_2 and O_2 can promote or decelerate the progression and duration of the wound healing process but H_2O_2 can reach critically high concentrations and prohibit healing. The growth of fibroblasts was greatly enhanced by nanozymes dressing at H_2O_2 concentration of 50 µM (Hu *et al* 2017). (Fu and Wang 2011) prepared $ZnFe_2O_4$-graphene nanocomposite via a one-step hydrothermal method. The photocatalytic activity measurements demonstrated that the $ZnFe_2O_4$-graphene catalyst acted as photoelectrochemical degrader. The photoactivity was increased with $ZnFe_2O_4$ and graphene coupling system. In addition, $ZnFe_2O_4$ nanoparticles themselves possessed magnetic properties, which made the $ZnFe_2O_4$-graphene composite magnetically separable in a suspension system.

Similarly (He *et al* 2017) synthesized MnO_2 nanosheets and observed that colourless 3,3,5,5-tetramethylbenzidine (TMB) was oxidized to a blue product (oxTMB), with increase in absorbance at 650 nm. On the addition of ascorbic acid reduction of MnO_2 nanosheets into Mn^{2+} and decrease in absorbance of reaction mixture was observed. The proposed colorimetric sensor possessed many advantages, including high sensitivity and selectivity and could be applied for fruit, juice and pharmaceutical samples under optimum conditions showing detection limit of 62.81 nM for ascorbic acid (AA) in aqueous solutions.

Cao *et al* (2011) used Fe_2O_3 nanowires as an ideal electrode material for fabrication of glucose sensors as they possess peroxidase-like activity. Biocatalytic performance of glucose sensor towards oxidation of glucose was found to be in a response time <6s with sensitivity of 726.9 $\mu AmM^{-1}cm^{-1}$. Ascorbic acid and dopamine at their maximum physiological concentrations were found to be highly sensitive towards glucose oxidation. Dong *et al* (2014) described pH-dependent Co_3O_4 NPs which showed multienzyme activity. In alkaline and neutral conditions, Co_3O_4 NPs acted as catalase and SOD mimetics. Co_3O_4 NPs can catalyze H_2O_2 oxidizing substrate in acidic medium and showed mainly peroxidase-like activity. Co_3O_4 NPs acted better enzyme mimetics, as compared to Fe_3O_4 NPs. Their mechanism was evaluated by ESR method. An immunohistochemical assay proved that of Co_3O_4 NPs could be used as peroxidase mimic. $Co_3(PO_4)_2$ was used to detect superoxide anions released from living cells. There was no significant difference between ions or molecules like K^+, Na^+, SO_4^-, NO or H_2O_2.

Maddinedi and Mandal (2014) reported enzyme mimic activity of quininic acid stabilized copper oxide nanosheets (CuO nanosheets) which were used in catalyzing the oxidation of o-dianisidine in the presence of H_2O_2 giving a light brown coloured product. The activity was due to the reduction of H_2O_2 to H_2O due to CuO nanosheets catalyzing the reaction.\ K_m value (15.8 mm) observed from the steady state kinetics was found to be higher than HRP but satisfied the condition of substrate binding. $V_{max.}$value for these nanosheets was 7.6×10^{-7} Ms^{-1}.

Sharma and Mobin (2017) synthesized CuO:Graphene (CuO: GNS) composite as peroxidase mimic for the detection of H_2O_2 and free cholesterol. The synthesized CuO: GNS composite was investigated systematically for structural, morphological and functional aspects. The mechanism involved oxidation of free cholesterol in the presence of cholesterol oxidase. The nanocomposite acted as sensor with excellent detection sensitivity for cholesterol. The CuO: GNS was found to have better cytocompatibility than standalone CuO. CuO NPs based graphene oxide (CuO/GO) composites can be synthesized with the hydrothermal method at various hydrothermal temperatures. These composites were used in biosensing of glucose. It showed the best nonenzymatic biosensing behavior. It also showed stability, better reproducibility, selectivity and accurate measurement in samples. Thus

CuO/GO composites possessed many applications on nonenzymatic glucose biosensors.

An effortless strategy is proposed for the amalgamation of cubic $CoFe_2O_4$ ferrite–reduced graphene oxide nanocomposite sheets (rGO–CFs), utilizing poly(N-vinyl-2-pyrrolidone) as the reductant and stabilizer. The rGO–CFs worked as proficient peroxidase mimetics and was effectively applied for colorimetric test. The morphology and structure of the rGO–CFs were characterized by transmission electron microscopy, X-beam photoelectron spectroscopy, and X-ray diffraction. Altogether, the peroxidase-like activity of the rGO–CFs followed regular Michaelis–menten kinetics and demonstrated a decent liking to 3,3,5,5-tetramethyl benzidine. Under ideal conditions, the colorimetric measure indicated a lower detectabe limit (S/N = 3) of 0.3 μM when contrasted and that of other nanoparticle based colorimetric examines. Besides, the cubic nanostructured rGO–CFs displayed preferable strength over horseradish peroxidase when they were presented to arrangements with various solvents and temperatures. These magnificent properties made the cubic nanostructured rGO–CFs a perfect contender for a wide scope of potential applications as peroxidase mimetics (Hao et al 2013). β−cyclodextrins (β−CD)- based consideration buildings of $CoFe_2O_4$ attractive nanoparticles (MNPs) were arranged and utilized as catalysts for chemiluminescence (CL) framework utilizing the luminol–hydrogen peroxide CL response as a model. The as-arranged complexes were described by TGA (Thermo gravimetric anaysis), XRD (X-ray diffraction) and FT-IR. The oxidation response among luminol and hydrogen peroxide in essential media started CL. The impact of β−CD-based incorporation buildings of $CCoFe_2O_4$ attractive nanoparticles and exposed $CoFe_2O_4$ attractive nanoparticles on the luminol–hydrogen peroxide CL framework was researched. It was discovered that consideration buildings among β−CD and $CoFe_2O_4$ attractive nanoparticles could incredibly improve the CL of the luminol–hydrogen peroxide framework. The practicality of utilizing the proposed framework for hydrogen peroxide detecting was additionally explored. Exploratory outcomes demonstrated that the CL outflow power was direct with hydrogen peroxide focus in the scope of 1.0×10^{-7} to 4.0×10^{-6} mol L^{-1} with a detection limit of 2.0×10^{-1} mol L^{-1} under advanced conditions. The proposed strategy has been utilized to detect hydrogen peroxide in water samples successfully (He et al 2010).

Synergistic impacts assume a significant role in improving the catalytic activity for enzyme like reactions. Contrasted with individual nanomaterials, a framework comprising of numerous segments for the most part shows upgraded catalytic activity as an enzyme mimics. Thus the blend of $CuFe_2O_4/Cu9S_8/$ polypyrrole (PPy) ternary nanotubes acts as an effective peroxidase mimic through a three-step advance methodology including an electrospinning procedure, hydrothermal reacion and annealing treatment. The amazingly improved catalytic activity of $CuFe_2O_4/Cu9S_8/PPy$ ternary nanotubes as peroxidase mimics over individual $CuFe_2O_4$ nanofibers, $CuFe_2O_4/CuO$ composite nanofibers, $CuFe_2O_4/CuS$ composite nanofibers, and PPy materials has been reported, showing the nearness of a synergistic impact among the parts. Based on high synergist movement, a colorimetric sensor for the delicate detection of H_2O_2 and dopamine has been created (Yang *et al* 2017).

A novel fluorescent hydrogen peroxide (H_2O_2) sensor was created based on the peroxidase-like activity of cupric oxide nanoparticles (CuO NPs). These NPs viably catalyzed the deterioration of H_2O_2 into hydroxyl radicals. At that point, terephthalic acid was oxidized by hydroxyl radical to form an exceptionally fluorescent product. The direct scope of hydrogen peroxide evaluated to be 5.0×10^{-6}–2.0×10^{-4} M with a detection limit of 3.4×10^{-7} M. Also, this location framework empowered the detecting of analytes which can enzymatically produce H_2O_2. By coupling the oxidation of glucose or l-lactate catalyzed by their respective oxidase enzymes with terephthalic acid oxidation catalyzed by cupric oxide nanoparticles, sensitive tests of glucose and l-lactate with detection limit of 1.0×10^{-6} and 4.5×10^{-8} were reported. The effective uses of this methodology in human serum tests have also been demonstrated (Hu *et al* 2014).

A productive colorimetric biosensor for glucose based on peroxidase-like protein-Fe_3O_4 and glucose oxidase nanocomposites (NC) was reported. Contrasted with pristine MNPs, peroxidase-like casein-MNPs display great catalytic properties, dependability, dispersibility. Casein joined on MNPs eminently improved the affinity toward both TMB and H_2O_2, demonstrated by variety in the decided kinetic parameters. As low as 0.2 μM H_2O_2 can be recognized with a linear range from 0.5 μM to 200 μM. All the more significantly, the casein/MNP NC was additionally used to immobilize GOx and to build a glucose biosensor for the one-step detection of glucose. This strategy is basic, reasonable, profoundly delicate, and particular for glucose recognition, with a detection limit of 2.0 μM over a straight range from 3 μM to 1000 μM (Liu *et al* 2014).

A straightforward and proficient colorimetric biosensing for hydrogen peroxide and glucose with peroxidase-like vitamin C (Vc) functionalized Fe_3O_4 magnetic nanoparticles (Vc Fe_3O_4 MNPs) as a catalyst is reported by Ren *et al* (2018). Contrasted with Fe_3O_4 MNPs and other different catalysts, $VcFe_3O_4$ MNPs showed prevalent catalytic properties. Kinetic investigations demonstrated that vitamin C joined on Fe_3O_4 MNPs enhanced the affinity toward H_2O_2. As low as 0.29 μmol/L H_2O_2 can be recognized with a wide direct range of 0.5—100 μmol/L ; also, as low as 0.288 μ mol/L glucose can be identified with a linear range of 0.5—20 μmol/L glucose. The discovery strategy was exceptionally specific in detecting H_2O_2 and glucose. The power of $VcFe_3O_4$ MNPs rendered them appropriate for wide running applications.

Porous manganese oxide/manganese ferrite ($MnO_x/MnFe_2O_4$) NC exhibited dual enzyme like activity towards H_2O_2 oxidation and selective oxidation of ketoses. The nanozyme exhibited oxidase-like activity by catalyzing the amplex red (AR) oxidation in the presence of dissolved oxygen to give fluorescent resorufin. The NC showed catalytic activity towards the selective oxidation of ketoses followed by the formation of H_2O_2. Since the NC did not catalyze the oxidation of aldose sugars, such as glucose and mannose, thus the catalyst is highly selective and sensitive for fructose detection with a detection limit 32 μM (Wu *et al* 2019).

γ-Fe_2O_3 nanoparticles (NPs) fabricated through single-source forerunner approach for colorimetric estimation of human glucose level was reported. The γ-Fe2O3 NPs, having cubic morphology with a normal molecule size of 30 nm, showed successful peroxidase-like activity through the catalytic oxidation of chromogenic peroxidase substrate 3,3′,5,5′-tetramethylbenzidine (TMB) within the presence of H_2O_2 delivering a blue-shaded solution. Based on this response, a straightforward, modest, exceptionally sensitive and selective colorimetric technique for estimation of glucose utilizing γ-Fe_2O_3/TMB/glucose–glucose oxidase (GOx) framework in the linear range from 1 to 80 μM with identification point of confinement of 0.21 μM was developed. The proposed glucose sensor shows quicker reaction, great strength, reproducibility and hostile to impedance capacity. Based on this reaction. Glucose level in human blood and urine can also be monitored (Mitra et al 2014).

A nanostructured multicatalyst framework comprising of Fe_3O_4 nanoparticles (MNPs) as peroxidase mimetics and an oxidative compound captured in large-pore-sized mesoporous silica has been produced for helpful colorimetric detection of biologically significant target molecules. The development of the nanocomposites (NC) starts with the fusion of MNPs on the dividers of mesocellular silica pores by impregnating $Fe(NO_3)_3.9\,H_2O$, trailed by the immobilization of oxidative enzymes. Glutaraldehyde crosslinking was utilized to forestall catalysts draining from the pores and prompted more than 20 wt % stacking of the enzyme. The oxidase in the NC creates H_2O_2 through its synergist activity for target atoms and in this way activates MNPs to change over chosen substrates into colored products. Utilizing this methodology, two distinctive biosensing frameworks were developed utilizing glucose oxidase and cholesterol oxidase and their investigative capacities were effectively checked by colorimetrically detecting the corresponding objective molecules with amazing selectivity, affectability, reusability, and stability. Future potential uses of this innovation run from biosensors to multicatalyst reactors (Kim *et al* 2011).

Another method for the detection of hydrogen peroxide (H_2O_2) and glucose using intrinsic peroxidase activity of Fe_3O_4 magnetic nanoparticles (MNPs) was reported by Gao *et al* (2011).In the sight of Fe_3O_4 MNPs as peroxidase mimetic catalyst, H_2O_2 was disintegrated into radical that could extinguish the fluorescence of CdTe QDs all the more productively and quickly. At that point, the oxidization of glucose by glucose oxidase was combined with the fluorescence extinguishing of CdTe QDs by H_2O_2 with Fe_3O_4 MNPs, which can be utilized to identify/detect glucose. Under the ideal response conditions, a straight relationship was built up between fluorescence intensity ratio I_o/I and concentration of H_2O_2 from 1.8×10^{-7} to 9×10^{-4} mol L^{-1} with a detection limit of 1.8×10^{-7} mol L^{-1}. A straight relationship was also set up between fluorescence intensity ratio I_o/I and concentration of glucose from 1.6×10^{-6} to 1.6×10^{-4} mol L^{-1} with an identification breaking point of 1.0×10^{-6} mol L^{-1}. The proposed strategy was applied to the detection of glucose in human serum tests with successful outcomes.

N,N′-di-carboxymethyl perylene diimides (PDI) have been utilized to functionalize Fe_3O_4 nanoparticles by means of an effortless course. The as-arranged PDI– Fe_3O_4 nanocomposites (NC) have been created as a novel chemical mimetic and have shown better peroxidase-like activitty to catalyze the oxidation of the peroxidase substrate 3,3′,5,5′-tetramethylbenzidine (TMB) within the presence of H_2O_2 than that of unadulterated Fe_3O_4 NPs just as other detailed Fe-based peroxidase mimics. Also, kinetic examination has uncovered that the synergist response was in concurrence with the run of Michaelis–Menten kinetics, and the PDI– Fe_3O_4 NC showed a higher affinity towards substrates, for example, TMB and H_2O_2. In addition, fluorescence information has shown that the synergist conduct can be surveyed by the electron transfer ability between H_2O_2 and TMB. In view of the benefits of PDI– Fe_3O_4 NC, for example, better dispersity, simple partition, upgraded synergist movement, affectability and selectivity for colorimetric detection of glucose, a colorimetric sensor was planned and utilized for the quick detection of H_2O_2 and glucose in a brief time frame (Chen *et al* 2017).

Song *et al* (2010) proved that carboxyl-modified graphene oxide ($GO^{-}COOH$) possessed intrinsic peroxidase-like activity which can catalyze substrate 3, 3, 5, 5-tetramethylbenzidine (TMB) in the presence of peroxide to produce a blue-colored reaction. A simple, colorimetric method was developed for glucose detection and used in buffer solution and fruit juice samples. They proved that intrinsic peroxidase activity of $GO^{-}COOH$ can be used in biotechnology. Kinetic studies proved that $GO^{-}COOH$ showed better catalytic activity than natural enzyme, horseradish peroxidase (HRP). For control of diabetes mellitus, it is important to calculate blood glucose level, for this purpose the number of glucose sensors had been reported. Out of them, horseradish peroxidase (HRP) was extremely used as sensors. In contrast to HRP, $GO^{-}COOH$ is low-cost, more stable to biodegradation, and less vulnerable to denaturation. These advantages made it more reliable to be used in environmental monitoring and medical diagnostics.

Su *et al* (2012) reported the inborn peroxidase like activity in the $ZnFe_2O_4$ magnetic nanoparticles (MNPs). $ZnFe_2O_4$ MNPs showed many advantages, for example, great stability, high catalytic efficiency, monodispersion, and quick partition over other peroxidase nanomimetics and horseradish peroxidase (HRP). $ZnFe_2O_4$ MNPs were utilized as a colorimetric biosensor for the identification of glucose level in urine. This technique is basic, cheap, profoundly delicate, and specific for glucose recognition utilizing glucose oxidase (GOx) and $ZnFe_2O_4$ MNPs with a direct range from 1.25×10^{-6} to 1.875×10^{-5}mol/L with a detection limit of 3.0×10^{-7} mol/L. The color change detectable by the unaided eyes dependent on the oxidation of 3,3′,5,5′-tetramethylbenzidine (TMB) is the standard for the detecting of urine glucose level.

Xu *et al* (2019)observed that meso-tetrakis(4-chlorophenyl)porphyrin functionalized $CuFe_2O_4/SiO_2$ NC (TClPP-$CuFe_2O_4/SiO_2$) exhibited the higher peroxidase-like activity as compared to $CuFe_2O_4/SiO_2$. The catalyst catalyzed the oxidation of the peroxidase substrate 3,3′,5,5′-tetramethylbenzidine (TMB) by H_2O_2 to give coloured product (oxTMB) observed by the naked eye. The above reaction was used for detection of H_2O_2 and colorimetric sensor for glucose in the range 8-80 μM and 5-100 μM respectively. Doped spinel ferrites $Co_xNi_{1-x}Fe_2O_4$ modified carbon paste electrodes (CPE) have been evaluated as artificial hydrogen peroxidase. Tailored electrochemical properties were observed using different Co/Ni molar ratios and $Co_{0.5}Ni_{0.5}Fe_2O_4$/CPE was observed to possess best electrocatalytic activity. Linear calibration curve was obtained over the wide range of 1.0×10^{-8} to 1.0×10^{-3} M with lower detection limit of 3.0×10^{-9} M. Increase in effective electroactive surface area increased electron transfer rate (Luo *et al*2013). The $NiCo_2O_4$ NPs fabricated three-dimensional graphene foam was also used as electrochemical electrode for the highly-sensitive and selective detections for calcium ion and glucose with limit upto 4.45 and 0.38 μM, respectively (Wu *et al* 2015).

$BiFeO_3$ nanoparticles (BFO MNPs) are utilized as a catalyst to build up a ultrasensitive technique for the detection of H_2O_2. It is discovered that BFO MNPs can catalyze the deterioration of H_2O_2 to create hydroxyl radicals, which thusly oxidize the feebly fluorescent benzoic acid to a firmly fluorescent hydroxylated product with a most extreme emission at 400 nm. This makes it conceivable to sensitively measure traces of H_2O_2. Under ideal conditions, the fluorescence intensity is seen to be well directly corresponded with H_2O_2 concentration from 2.0×10^{-8} to 2.0×10^{-6} mol L^{-1} with an identification point of confinement of 4.5×10^{-9} mol L^{-1} (S/N = 3). Also, a specific technique for glucose detection is created by utilizing both glucose oxidase and BFO MNPs, which has a straight range for glucose concentration from 1.0×10^{-6} to 1.0×10^{-4} mol L^{-1} with a detection limit of 5.0×10^{-7}mol L^{-1}. These new techniques have been effectively applied for the detection of H_2O_2 in water and glucose in human serum tests (Luo *et al* 2010).

$ZnFe_2O_4$ showed intrinsic peroxidase-like activity by catalyzing the oxidation of o-phenylenediamine in the presence of H_2O_2 resulted into yellow coloured product (oxOPD). The oxOPD quenched the fluorescence of boron and nitrogen co-doped CDs (B,N-CDs), thus, the fluorescence intensity ratio (I_{556}/I_{430}) was utilized for quantitative analysis of H_2O_2 and H_2O_2-involved metabolites like uric acid (UA) and glucose. The colorimetric detection limit for H_2O_2, UA and glucose are 0.09, 0.9, and 0.9μM, respectively, and 0.1, 8, and 1μM using ratiometric fluorescent sensing. This model reaction provides potential applications to detect glucose and UA in human serum (Xiao *et al* 2018).

Chen *et al* (2015) reported that poly(sodium styrene sulfonate)-functionalized graphene nanosheets (PSS-GN) could mimic peroxidase activity which might be due to the stronger binding between substrate TMB and negatively charged PSS. The PSS-GN NCs could detect glucose and H_2O_2 by colorimetry in the range of 0.005-1mM and 0.006-0.4 mM respectively. For enzyme less determination of glucose, graphene oxide-molecular imprinted Polymer (GO-MIP) based electrochemical sensor was reported by Alexander (2017). The proposed electrode exhibited superior electrocatalytic activity for glucose oxidation at optimized conditions with minimum detection limit of 0.1 nM within~ 2 min. The electro-chemical response of GO-MIP based sensor was linearly proportional to the glucose concentration. The results acquired from GO-MIP based electrodes in human blood were comparable to commercially available glucose monitors.

Cu–hemin metal-natural structures (MOFs) were reported to possess peroxidase-like activity. The fabricated Cu–hemin MOFs were characterized by different strategies, for example, transmission electron microscopy, scanning electron microscopy, X-ray powder diffraction, Fourier transfer infrared spectroscopy, UV–visible absorbance spectra, etc. The outcomes demonstrated that the Cu–hemin MOFs appeared as though a ball-blossom with a normal breadth of 10 μm and gave an enormous explicit surface region. The Cu–hemin MOFs having peroxidase-like activity was utilized to catalyze the peroxidase substrate of 3,3,5,5-tetramethylbenzidine within the presence of H_2O_2, which was utilized to distinguish H_2O_2 quantitatively with the direct linear range from 1.0 μM to 1.0 mM and the detection limit was 0.42 μM. Besides, with the extra assistance of glucose oxidase, a delicate and specific technique to identify glucose was created by utilizing the Cu–hemin MOFs as catalyst and the direct range was from 10.0 μM to 3.0 mM and detection limit was 6.9 μM (Liu *et al* 2016).

MoS_2 nanoflakes (MoS_2 NFs) with a breadth of ∼400 nm were fabricated by an easy one-pot hydrothermal process and the NFs displayed natural peroxidase-like activity. Subsequent to being altered by generally utilized biocompatible surfactants including polyvinylpyrrolidone (PVP), polyacrylic corrosive (PAA), polyethyleneimine (PEI), and cysteine (Cys), the peroxidase-like synergist exercises of MoS_2 NFs were researched by utilizing 3,3′,5,5′-tetramethylbenzidine (TMB) and 2,2′-azino-bis(3-ethylbenzothiazoline-6-sulfonic acid)diammonium salt (ABTS) as chromogenic substrates. Contrasted with the polymer changed MoS_2 NFs, Cys functionalized MoS_2 NFs showed a high catalytic acivity toward H_2O_2 within the presence of TMB or ABTS. Strikingly, another peroxidase-like synergist response component was proposed dependent on the arrangement of a transient province of Cys– MoS_2NFs containing H_2O_2 and ABTS, and the synergist response could happen in light of the fact that the Cys on the outside of the MoS_2 NFs filled in as an electron move connect among H_2O_2 and ABTS. In light of this discovering, we additionally settled a stage for colorimetric discovery of $H_2O_2$and glucose utilizing Cys— MoS_2NFs as a peroxidase substitution. The limit of detection (LOD) was resolved to be 4.103 μmol L^{-1} for H_2O_2, and the direct linear range (LR) was from 0 to 0.3 mmol L^{-1}. The LOD for glucose was 33.51 μmol L^{-1} and the LR was from 0.05 to 1 mmol L^{-1}, which is appropriate for biomedical conclusion (Yu *et al* 2018).

A colorimetric technique for the detection of Hg (II) ions by utilizing the peroxidase-like activity of MoS_2 nanosheets (MoS_2-NSs) was developed by Lu *et al* (2016). These were set up by sonication-prompted shedding of mass MoS_2 precious stones in fluid surfactant arrangement. The MoS_2-NSs were found to act as peroxidase mimic that is capable for oxidizing the chroogenic substrate 3,3′,5,5′-tetramethylbenzidine (TMB) within the sight of hydrogen peroxide (H_2O_2) to give a blue product with maximum wavelength at 652 nm. The expansion of Hg(II) unequivocally quickens the energy of this response. It is demonstrated that the protein emulate has a high liking for TMB and a lower pseudo-Michaelis-Menten steady. The animating impact of Hg(II) is genuinely affected by the difference in surface charge. The utilization of nanosheets secured with (adversely charged) polystyrene sulfonate brings about abatement in the arrangement of blue color, while those secured with (cationic) poly(diallyldimethyl ammonium) particles cause a little increment. Under ideal conditions, the peroxidase-like movement of MoS_2-NSs is influenced by Hg(II) in the linear range of 2.0 to 200 μM.

Co_3O_4 NPs fabricated crumpled graphene microspheres (CGM) were evaluated for their potential as enzyme mimics. Peroxidase enzyme was taken as model enzyme and detection of ascorbic acid by synthesized NPs and nanohybrids was studied. The nanohybrids possessed superior catalytic activity than Co_3O_4 and CGM due to increase in specific surface, that led to more adsorption of TMB and H_2O_2 and rapid electron transfer between the substrate and nanohybrid. The presence of ascorbic acid tempted two electron reduction of oxTMB to TMB with fading of blue colour. The nanohybrids were effective as peroxidase mimic in pH range 1.0 – 12.0 and temperature 15-80°C and above 92.5% activity was retained even after one month storage thus exhibiting long term storage stability (Fan *et al* 2017).

Due to the synergistic effect between the CoS and $CoFe_2O_4$, the $CoFe_2O_4$/CoS NCs showed enhanced peroxidase like activity than either the $CoFe_2O_4$ nanotubes or CoS NPs alone for the detection of dopamine. Detection was based on the basis of ability of dopamine to promote the reduction of o-TMB to TMB with fading of the blue color with a wide range (0–50 μM) and low detection limit = 0.58 μM (Yang *et al* 2018).

Table 2.2: Detection of various metabolites by different NPs

Sr. No.	Nanozyme	Metabolite detected	Reference
1.	$NiFe_2O_4$	Glucose	Su *et al* 2015
2.	CeO_2	Glucose	Liu *et al* 2015
3.	$ZnFe_2O_4$	Glucose	Su *et al* 2012
4.	Fe_2O_3 nanowires	Glucose	Cao *et al* 2011
5.	MnO_2 nanosheets	Ascorbic acid	He *et al* 2017
6.	$Co_3(PO_4)_2$	Superoxide anions	Dong *et al* 2014
7.	CdS	Hg^{2+}	Yang *et al* 2016
8.	$MnO_x/MnFe_2O_4$	Fructose	Wu *et al* 2019
9.	$ZnFe_2O_4$	Uric acid	Xia *et al* 2018
10.	$CuFe_2O_4/CuS$	Dopamine	Yang *et al* 2017

Thus, it can be concluded that ferrite NPs and their nano-composites have been recently used as enzyme mimics for the detection of different metabolites. Literature review showed that enzyme mimic activity is influenced by the surface interactions and surface area of contact. The present studies pertaining to synthesis of CTAB coated $MgFe_2O_4$ NPs for hydrogen peroxide and glucose sensing are important in understanding enzyme mimic activity of these materials.

CHAPTER – III

MATERIALS AND METHODS

This chapter gives details about the experimental procedures used during the course of the investigation. The different chemicals used, methods, characterization tools employed for the synthesis of magnesium ferrite nanoparticles ($MgFe_2O_4$ NPs), Cetyl trimethyl ammonium bromide (CTAB) coated $MgFe_2O_4$ are discussed.

3.1 Chemicals and reagents used

The list of different chemicals used for the synthesis of NPs and peroxidase like activity is shown in Table 3.1

Table 3.1: List of chemicals used

S. No.	Chemicals
1.	Magnesium nitrate (hexahydrate) ($Mg(NO_3)_2 . 6 H_2O$)
2.	Ferric Nitrate (Nonahydrate) ($Fe(NO_3)_3.9H_2O$)
3.	Citric Acid monohydrate ($C_6H_8O_7$)
4.	Ammonium hydroxide (NH_4OH)
5.	Cetyl trimethyl ammonium bromide (CTAB)
6.	Hydrochloric acid (HCl)
7.	Sodium hydroxide (NaOH)
8.	o-dianisidine dihydrochloride
9.	30 % Hydrogen Peroxide (H_2O_2)
10.	Glucose oxidase

3.2 Instrumentation tools

Different characterization tools employed to study the phase purity, magnetic properties, particle size, functional groups and surface morphology along with the model of the instruments used are given in Table 3.2

Table 3.2: List of various Instruments and their models

S. No.	Instruments	Model	Place
1.	X-ray Diffraction (XRD)	CuKα radiations ($\lambda = 1.5404A^{o}$) with a Panalytical X pert Pro	Central research facility, IIT, Ropar
2.	Fourier Transform Infrared spectroscopy (FT-IR)	Thermo Nicolet 6700 Fourier Transform Infrared Spectrometer	Central Instrumentation Laboratories (CIL), Panjab University, Chandigarh
3.	Transmission electron microscopy (TEM)	Hitachi Hi-7650 at 100 kV accelerate voltages in HC mode	EMN Lab, Punjab Agricultural University, Ludhiana
4.	Brunauer–Emmett–Teller (BET)	Quanta chrome Autosorb 1C	Material Analysis and Research centre, Banglore
5.	Vibrating sample magnetometer (VSM)	Vibrating Sample Magnetometer(VSM) (PAR 155)	Central Instrumentation Facility, IIT Roorkee
6	UV–Visible spectrophotometer	Shimadzu (UV-1800) UV spectrophotometer	Central Laboratory, Department Of Chemistry Punjab Agricultural University, Ludhiana

3.3 Synthesis of nanoparticles

3.3.1 Synthesis of magnesium ferrite ($MgFe_2O_4$)

$MgFe_2O_4$ nanoparticles (NPs) were synthesized by using sol-gel method employing citric acid as a complexing agent (Kaur *et al* 2015). Ferric nitrate (0.032 moles) and magnesium nitrate (0.016 moles) with molar ratio 2:1 were dissolved in 20 mL distilled water and then 0.072 moles of citric acid was added to the reaction mixture. Role of citric acid is to make complex with the metal ions which helps in their homogeneous distribution in the mixture. The above mixture was converted into sol by addition of ammonium hydroxide and pH of solution was neutralized. The gel was obtained by magnetically stirring the mixture at 60°C for 3-4 hours. The gel was dried at 200 °C for 3 hours. Finally the dried gel was calcined at 300 °C for 3 hours to get $MgFe_2O_4$ NPs as final product.

Pictorial representation of the synthesis of magnesium ferrite is shown in Scheme 3.1

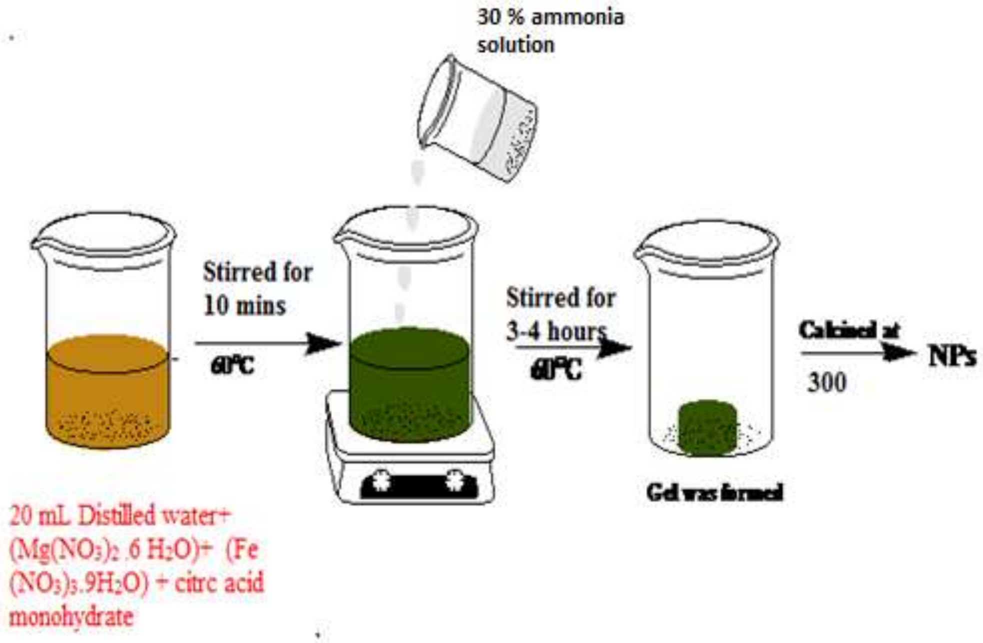

Scheme 3.1: Synthesis of magnesium ferrite nanoparticles using sol-gel method

3.3.2 Synthesis of Cetyl trimethyl ammonium bromide (CTAB) coated nanoparticles.

CTAB@$MgFe_2O_4$ NPs were prepared by sonication method. These NPs were prepared in different w/w ratios that are 1:2, 1:1, 2:1.

1g of $MgFe_2O_4$ NPs synthesized by sol-gel method were added in 20 ml of distilled water. 0.5g CTAB was added in 20 ml D.W. Both the solutions were subjected to sonication for 30 minutes separately. After 30 mins, solution containing NPs and CTAB were mixed thoroughly and again subjected to sonication for 30 minutes. NPs were filtered out using centrifuge tube, then they were dried for 2 days and CTAB@$MgFe_2O_4$in 1:2 (w/w) were obtained and labelled as E-2. In the similar way CTAB amount was increased to 1.0 and 2.0 g and the resultant CTAB coated NPs were labelled as E-3 and E-4.

3.4 CHARACTERIZATION

3.4.1 'XRD'parameters'

The lattice constant 'a' tells about the distance between unit cells in a crystal lattice, which is calculated by the relationship given below:

$$a = d(h^2 + k^2 + l^2)^{1/2}$$

where h, k, l are integers which determine lattice planes, and 'd' is inter lamaller spacing.

$$\text{Density} = \frac{8M}{Na^3}$$

Where

M = Molecular weight

N = Avogadro's number (6.023×10^{23})

Scherrer's relationship (Cullity 1978) was used to calculate the average particle size (D) as follows:

$$D = \frac{0.9\,\lambda}{d\ \mathrm{Cos}\theta}$$

Where,

d is full width at the half maximum

Ɵ is Bragg's diffraction angle.

Physical density is calculated as:

$$\rho_{\mathrm{sample}} = \frac{(W_2 - W_1) \times \rho_{\mathrm{xylene}}}{(W_2 - W_1) + (W_4 - W_3)}$$

Where,

W_1 = Weight of the specific gravity bottle

W_2 = Weight of the specific gravity bottle + sample

W_3 = Weight of the specific gravity bottle + sample + xylene

W_4 = Weight of the specific gravity bottle + xylene

ρ_{xylene} = Density of xylene

ρ_{sample} = Density of sample

The porosity percentage of the synthesized nanoparticles was estimated from following equation (Kaur *et al* 2012):

$$\mathrm{Porosity}\ (\%) = \left[1 - \frac{d_{\mathrm{exp}}}{d_{\mathrm{XRD}}}\right] \times 100$$

3.4.2 Transmission electron microscopy (TEM)

To evaluate the particle size of samples, TEM technique was used. The sample was prepared in Distilled water by sonicating the mixture for 1 hour. Copper grid was used to mount the samples and to support the sample; because copper is conducting stable and does not interfere with the image. A drop of formulated dispersion was mounted on the copper grid and was dried in the oven after which the sample was analyzed under TEM.

3.4.3 Magnetic parameters

Hysteresis curve is the graph between the magnetic field (O_e) and intensity of magnetization or flux density (I or B). By eliminating external magnetic field for the ferromagnetic materials, i.e. H = 0, the magnetic moment of some domains continues to be oriented in the applied direction of magnetizing field which results into a residual magnetism. Once magnetized, the magnet will remain magnetized for an indefinite period. It requires either heat or a magnetic field in the opposite direction for demagnetization.

(i) When magnetizing field (H) was increased, the intensity of magnetization or flux density (I, B) also increases and reaches to an extreme value denoted by curve OA. On further increasing the value of H, the value of B remains constant. This maximum value is known as the saturation value and the point A as saturation point.

(ii) When H is reduced, I is also decreased but is not zero when, H = 0. The magnetization retained by the magnetic material even when H was reduced to zero is called the residual magnetism or retentivity represented by the curve OB.

(iii) When the flow of magnetic field H is inverted, the magnetization decreases and for a particular value of H, denoted by H_c, it became zero i.e., $H_c = OC$ when $I = 0$. This value of H is known as coercivity.

(iv) The course of demagnetising a material entirely by employing magnetising field in a negative direction so that B becomes zero is defined as coercivity. Coercivity estimates the hardness or softness of a magnetic material.

The process of lagging behind the magnetization with respect to the magnetic field is known as hysteresis.

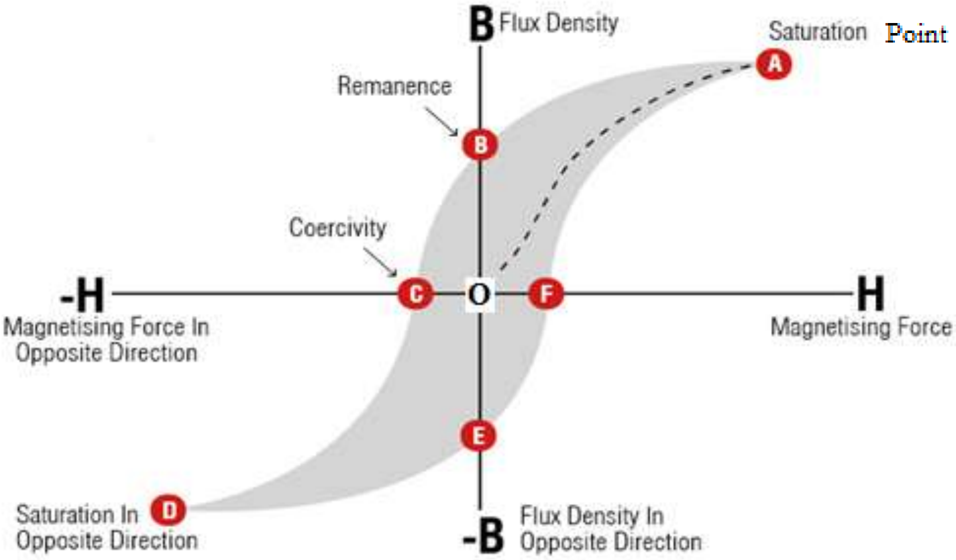

Figure 3.1: Typical hysteresis loop showing the magnetic parameters

3.5 Peroxidase mimic activity evaluation

Peroxidase like activity of synthesized NPs was evaluated by Shannon *et al* (1966) method. Peroxidase catalyzes oxidation of substance using hydrogen peroxide. o-dianisidine dihydrochloride is used as a substrate by measuring the increase in absorbance at 435 nm. The reaction mixture consisted of 20 mL of 2 mM substrate solution (12.7 mg in 20 mL water), 5 mg of synthesized NPs and hydrogen peroxide. The control only contained 20 mL of the substrate.

3.5.1 Comparison of Peroxidase like activity of synthesized NPs

The synthesized NPs were compared by using 2 mM o-dianisidine dihydrochloride solution with pH < 7.0. 20 mL of 2 mM substrate solution of pH < 7.0 was taken in the beaker. To the above solution, 5 mg of synthesized $MgFe_2O_4$/CTAB@$MgFe_2O_4$ (w/w 1:1, 1:2, 2:1) was added. Change in absorbance was noted after 10 min at 435 nm on UV-Visible spectrophotometer.

3.5.2 Effect of pH

The effect of pH on peroxidase like activity was observed by varying pH from 1.0-9.0. 20 mL of 2mM substrate solution of pH varied from 1.0-9.0 was taken into the beaker. pH was varied using 0.1 N HCl and 0.1 N NaOH. To the above solution, 5mg of synthesized CTAB@$MgFe_2O_4$ (w/w 1:1) NPs were added. Change in absorbance was noted after 10 min at 435 nm on UV-Visible Spectrophotometer. The optimum pH values obtained in this procedure were used in all subsequent experiments.

3.5.3 Effect of temperature

The effect of temperature on peroxidase like activity was observed by varying temperatures from 15^o-45^oC. 20 ml of 2 mM o-dianisidine dihydrochloridesolution (at optimum pH) was taken in the beaker. To the above solution 5 mg of synthesized NPs were added. The above solution was studied at different temperatures ranging from 15-45^0 C. After 10 min absorbance was noted at 435 nm.

3.5.4 Effect of contact time

The effect of contact time on peroxidase like activity was studied over 20 min at 2 min intervals. 20 ml of 2 mM substrate solution (at optimum pH) was taken in the quartz cuvette. To the above solution added 5 mg of synthesized NPs. Change in absorbance was noted at 2 min interval for 20 min at 435 nm on UV-Visible Spectrophotometer.

3.5.5 Effect of substrate and NPs dose

The effect of substrate dose on peroxidase like activity was studied by varying substrate dose from 1-6 mM. 20 ml of o-dianisidine dihydrochloride solutions with concentration varying from 1-6 mM was added in different beakers and pH was adjusted to optimum value. To the above solution were added 5mg of synthesized NPs. Change in absorbance was noted after 10 min at 435 nm on UV-Visible Spectrophotometer.

The effect of NPs dose on peroxidase like activity was studied by varying NPs dose from 1-6 mg. 20 mL of 2mM substrate solution with concentration of NPs varied from 1-6 mg was added in different beakers and pH was adjusted to optimum value. Change in absorbance was noted after 10 min at 435 nm.

3.6 Kinetic Studies

The reaction kinetics for the catalytic oxidation of o-dianisidne dihydrochloride by NPs were determined by using Lineweaver-Burk plot, which helps to calculate Michaelis-Menten constant (K_m) as follows:

$$\frac{1}{V} = \frac{K_m}{V_{max}[S]} + \frac{1}{V_{Max}}$$

Here,

V is initial velocity of the reaction.

V_{Max} is the maximum velocity of the reaction

[S] is the substrate concentration

K_m is the Michaelis-Menten constant (indicator of enzyme affinity for its substrate).

The concentration of o-dianisidine dihydrochloride was varied from 1mM to 6 mM to which 5 mg of NPs were added at optimized pH and absorbance change at 435 nm was monitored at 1 min intervals at room temperature for 5 min. The kinetic studies of the oxidation of o-dianisidine dihydrochloride in the presence of NPs were carried out by the method of initial rates by following the increase in absorbance at 435 nm. The rate constants were evaluated from

log $[A_o/(A_o-A_t)]$ versus time plot

Where, A_o and A_t are the absorbance values at an infinite time and at a time 't' respectively. To determine Michaelis menten constant and V_{max} plot was drawn between 1/V (y-axis) and 1/S (x-axis) having slope $K_m/V_{max.}$ and intercept $-1/K_m$ on X-axis .

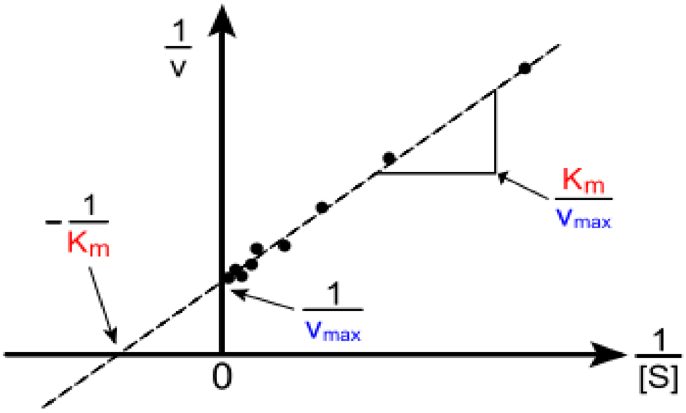

Fig. 3.2: Lineweaver Burk Plot

The smaller value of K_m indicates the greater affinity between enzyme and substrate. Statistical analysis was done on the effect of pH, temperature, contact time and concentration of substrate on the peroxidase activity of synthesized NPs.

3.7 Detection of H_2O_2 and glucose based on CTAB@$MgFe_2O_4$ peroxidase mimics

For H_2O_2 detection: 100 µL CTAB@$MgFe_2O_4$ (0.25mg/mL), 2500 µL o-dianisidine dihydrochloride (2mM), and 1000 µL of different concentrations of H_2O_2 (i.e. 5,10,20,40,50,60,80,100,200,300 µM) were added to 6400 µL of solution of pH 3. The solution was incubated at 25°C for 10 min and the colour change was monitored using spectrophotometer.

Glucose detection was performed in the following steps: 1) GOx (200 μL, 1 mg mL^{-1}) and 1000 μL of different concentrations of glucose (i.e. 5,10,20,30,50,100,200,500, 1000,2000 μM) were incubated at 37ºC for 30 min to produce H_2O_2. 2) 100 μL CTAB@$MgFe_2O_4$ (0.25 mg mL^{-1}), 2500 μL o-dianisidine dihydrochloride (2 mM) were added in 6200 μL of distillled water of pH 3.0. Both these solutions were mixed and incubated at 25 ºC for 10 min and then used for adsorption spectroscopy.

Solution of pH 3.0 was chosen for H_2O_2 and glucose detection because of its close approximation with the biological solutions and little difference between enzyme mimic activities of CTAB@$MgFe_2O_4$ NPs at solution of pH 1.0 and pH 3.0.

3.8 Statistical analysis

All experiments were carried out in triplicates and the results were expressed as mean ± standard deviation. To estimate significance difference between the peroxidase mimic activity of different prepared one way analysis of variance (ANOVA) was used. The results were considered statistically significant at $p < 0.05$.

.

CHAPTER – IV

RESULTS AND DISCUSSIONS

The present study pertained to the synthesis of magnesium ferrite nanoparticles ($MgFe_2O_4$) by sol gel method denoted as E-1 and Cetyl trimethyl ammonium bromide (CTAB) coated $MgFe_2O_4$ NPs in different w/w ratios 1:2, 1:1, 2:1 by ultrasonication route designated as E-2, E-3, and E-4. The as fabricated NPs were evaluated for their potential as enzyme mimic for peroxidase like activity and sensing of hydrogen peroxide and glucose. The results obtained are discussed under the following headings:

4.1 X-Ray diffraction (XRD) analysis

This analysis was used to identify the phase purity of as synthesized NPs. X-ray diffractograms of $MgFe_2O_4$ and CTAB@$MgFe_2O_4$ (Fig. 4.1) displayed well defined peaks. The various XRD parameters such as X-ray density, lattice constant, average crystalline size, experimental density and percentage porosity are listed in Table 4.1. The diffractions patterns of $MgFe_2O_4$NPs comprise of peaks corresponding to crystallographic planes (2 2 0), (3 1 1), (4 0 0), (4 2 2), (5 1 1). All the results of the diffraction patterns were in accordance with reported values (Kaur and Kaur 2014, Spiers *et al* 2004). The mean crystallite size was estimated using Scherrer's formula from the half width of the most intense peak of the diffractogram (Cullity 1976). The size of the NPs was found to be in the range of 7-12 nm. Decrease in size of NPs is observed on coating with CTAB from 11.0 nm to 7.0 nm. Lattice constant (nm) for $MgFe_2O_4$ NPs obtained using the XRD data was found to be 0.8402 nm. Singh and Venkataraju (2018) also synthesized $MgFe_2O_4$ NPs having lattice constant values of 0.8391 nm. In E-3, the peaks were widened and increased FWHM was observed, confirming decrease in average particle size relative to pristine $MgFe_2O_4$ NPs. These results proposed that the interplanar spacing increased leading to the decrease in size of the particle. X-Ray density, lattice constant and average particle size for all the samples was shown in (Table. 4.1).

Table 4.1: XRD parameters of synthesized NPs

Material Code	Nanoparticles (NPs)	Lattice constant (Å)	X-Ray density (g/cc)	Average particle diameter (nm)
E-1	$MgFe_2O_4$	8.4017	4.48	11.0
E-2	CTAB@$MgFe_2O_4$ (1:2)	8.3623	8.11	10.0
E-3	CTAB@$MgFe_2O_4$(1:1)	8.3812	8.19	7.0
E-4	CTAB@$MgFe_2O_4$ (2:1)	8.3918	8.22	9.0

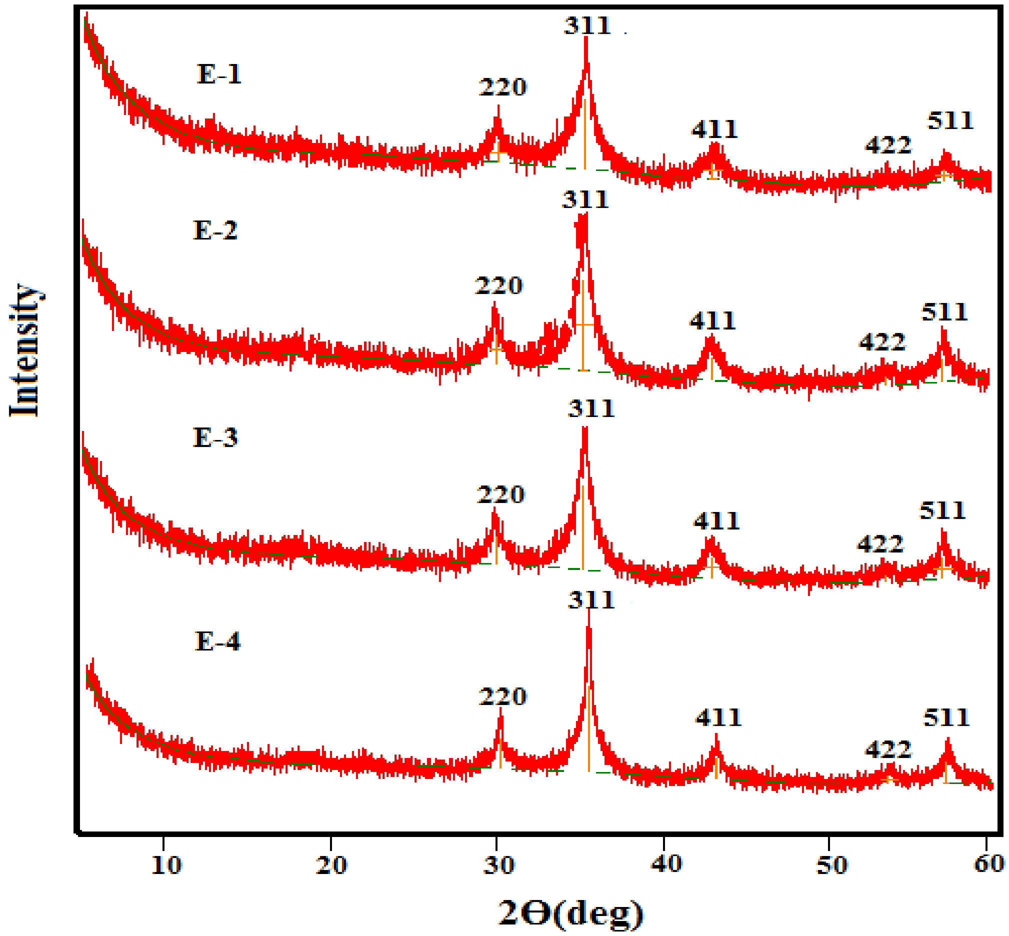

Fig. 4.1: X-Ray diffraction patterns of E-1, E-2, E-3 and E-4

4.2 Fourier Transformation Infrared (FT-IR) Study

The coating of CTAB on the $MgFe_2O_4$NPs was investigated by FT-IR spectra. Fig. 4.2 represents FT-IR spectra of $MgFe_2O_4$ NPs and CTAB coated NPs (E2, E3, and E4). In the spectrum of pristine NPs there are six characteristics bands. Bands at 3424 cm^{-1} and 1633 cm^{-1} account for stretching and bending vibrations of OH groups of water molecules respectively (Thankachan *et al* 2013). Formation of spinel structure was confirmed by band at 431 cm^{-1} and 578 cm^{-1} while the former accounted for vibration of tetrahedral complex the later corresponded to the M-O (s) of octahedral complex (Pradeep *et al* 2008).

FT-IR spectrum of CTAB@$MgFe_2O_4$NPs(E-3, 1:1 w/w) shows all the peaks of pristine NPs and two additional peaks are present at around 2800 and 2900cm^{-1} due to anti symmetric and symmetric stretching of $-CH_2-$respectively. A narrow band at 1384 cm^{-1} is characteristic of $-CH_3$ symmetrical deformation. FT-IR spectra of E-2 and E-4 also showed the peaks of CTAB in the above described region but transmittance differs in all the three samples (Kuppayee *et al* 2012).

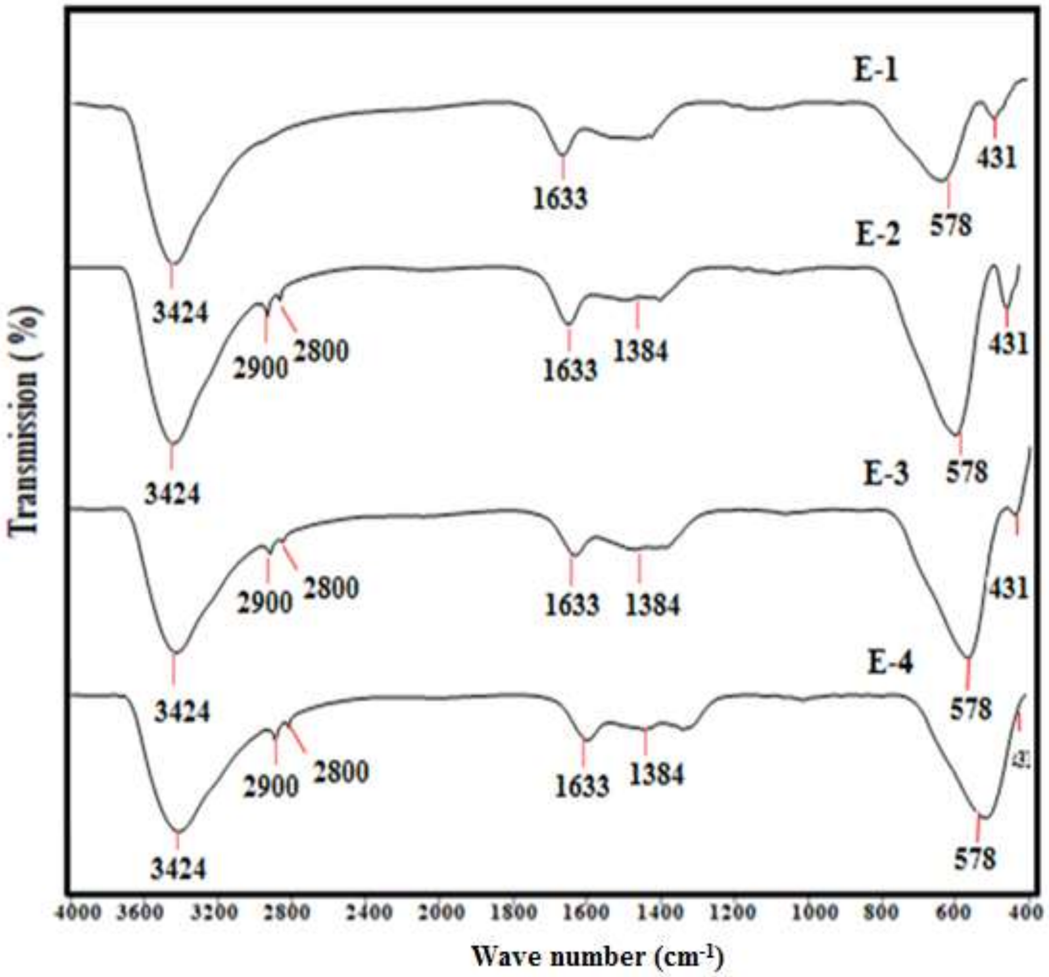

Figure 4.2 FT-IR spectra of E-1, E-2, E-3, and E-4

4.3 Transmission Electron Microscopy (TEM)

The topographical features, particle size and aggregation behaviour of as fabricated NPs was analyzed by TEM analysis using aqueous dispersion of synthesized compounds. TEM micrographs and histograms of E-1, E-2, E-3, and E-4 respectively were represented in Fig. 4.3(a) and 4.3(b) respectively. TEM micrographs of E-1 show agglomerated particles and from histogram its particle size is in accordance with XRD results. E-2, E-3 shows NPs tend to separate due to addition of CTAB. Garg *et al* (2018) also observed similar trend on surfactant coated Fe_2O_3 NPs.

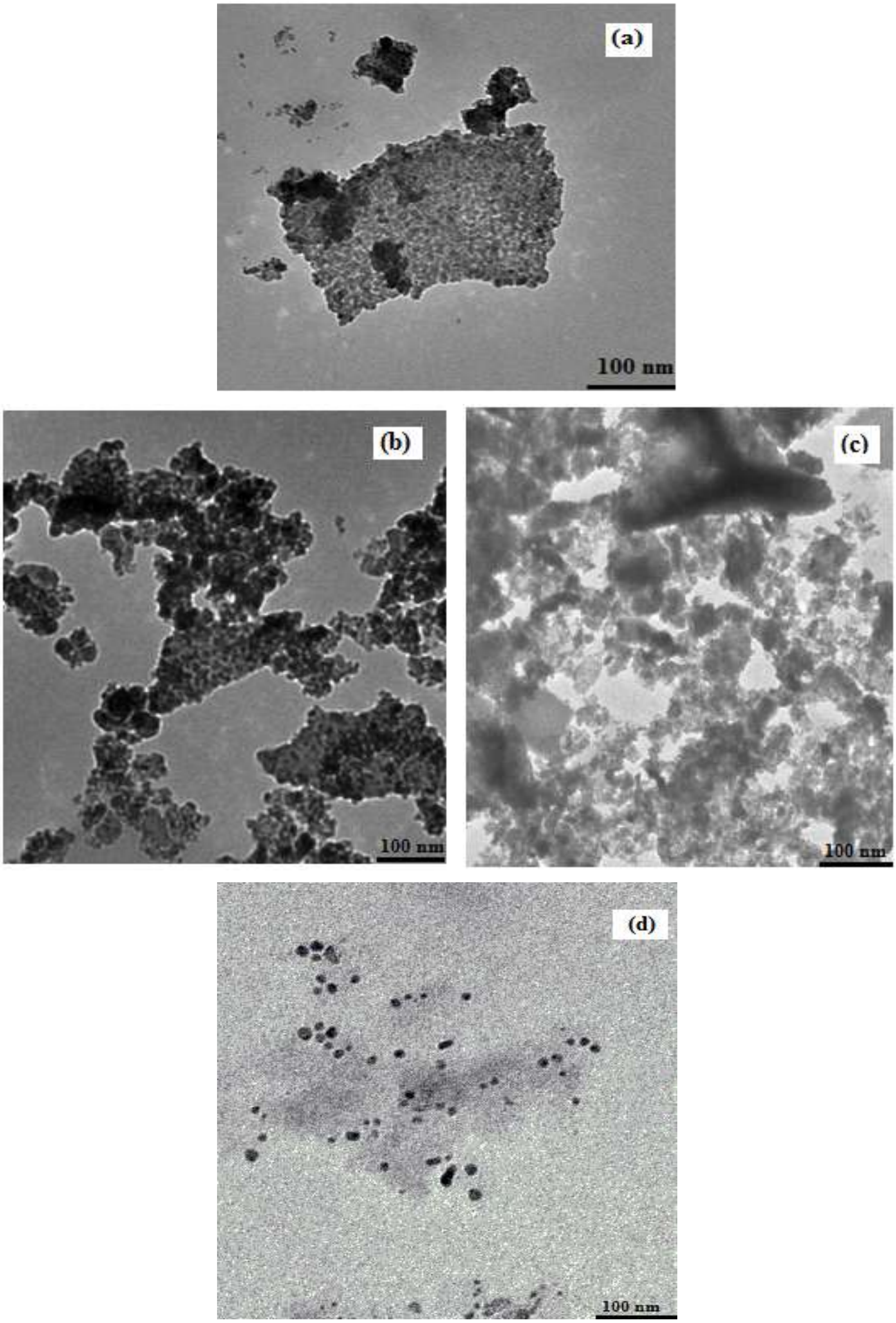

Fig. 4.3(A): Electron micrographs of (a) E-1 (b) E-2 (c) E- 3 (d) E-4

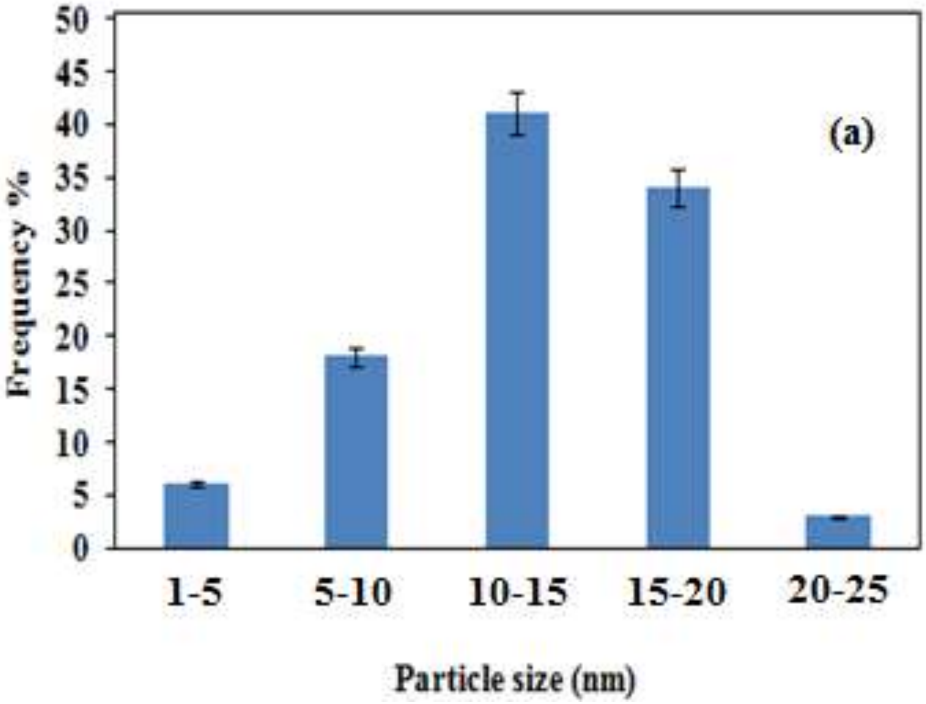
(a)
Frequency %
0
5
10
15
20
25
30
35
40
45
50
1-5
5-10
10-15
15-20
20-25
Particle size (nm)

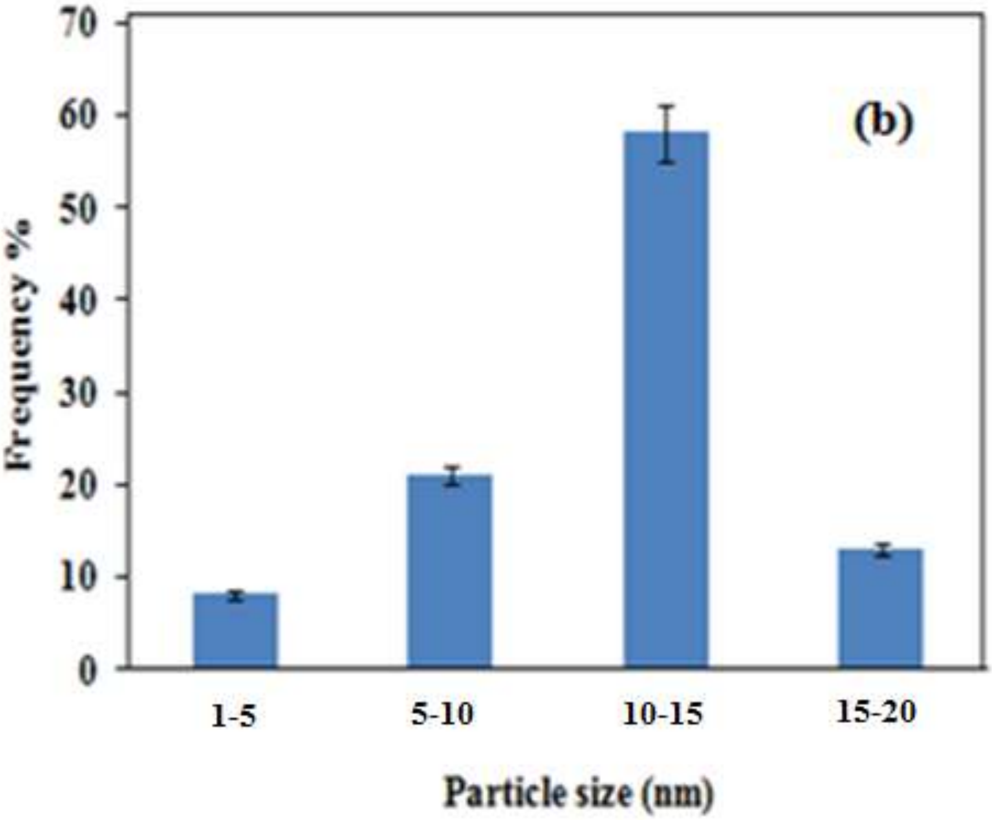
(b)
Frequency %
0
10
20
30
40
50
60
70
1-5
5-10
10-15
15-20
Particle size (nm)

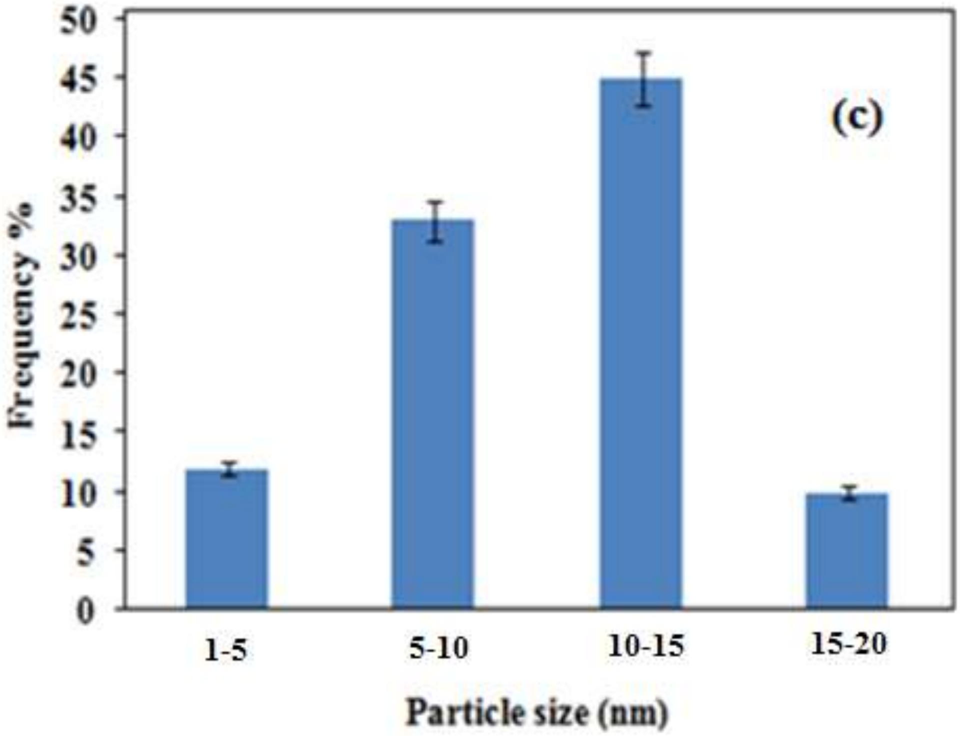

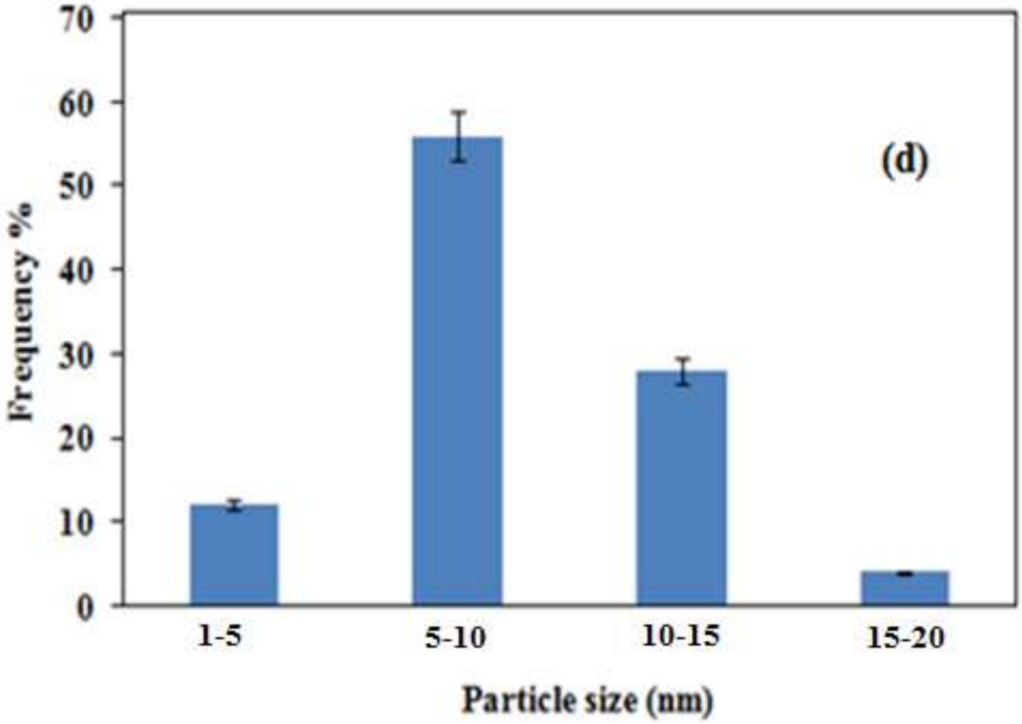

Fig. 4.3(B): **Transmission Electron Microscopy histogram of particle size distribution (a) E-1 (b) E-2 (c) E- 3 (d) E-4**

4.4 Brunauer-Emmet-Teller (BET) surface area study

Surface area of the synthesized materials were evaluated using nitrogen adsorption-desorption measurements. The N_2 sorption isotherms and corresponding pore size distribution curves of the samples are shown in Fig: 4.4 (a, b, c, d). According to IUPAC classification, these isotherms are designated as type IV which indicate that the structure is mesoporous with a broad hysterisis loop belonging to H1 type. The BET surface area of E-1, E-2, E-3 and E-4 are 58.81, 60.36, 78.29 and 73.15 m^2/g, respectively. The agglomeration occurring due to strong Vander Waals forces of attraction lowers the surface area of pristine NPs. On addition of CTAB, NPs get separated and their surface area increased till 1:1. Further increase in the concentration of CTAB didn't bring any change in the surface area (Garg *et al* 2018). Thus E-3 showed maximum surface area which was in agreement with enzyme mimic activity results. The parameters like pore volume, pore diameter and surface area of both the samples are listed in table 4.2.

Table 4.2 BET surface area parameters of NPs.

Compound	**Surface area (m^2/g)**	**Pore volume (cc/g)**	**Pore diameter (nm)**
E-1	58.81	0.087	3.565
E-2	60.36	0.093	3.587
E-3	78.29	0.114	3.602
E-4	73.15	0.101	3.582

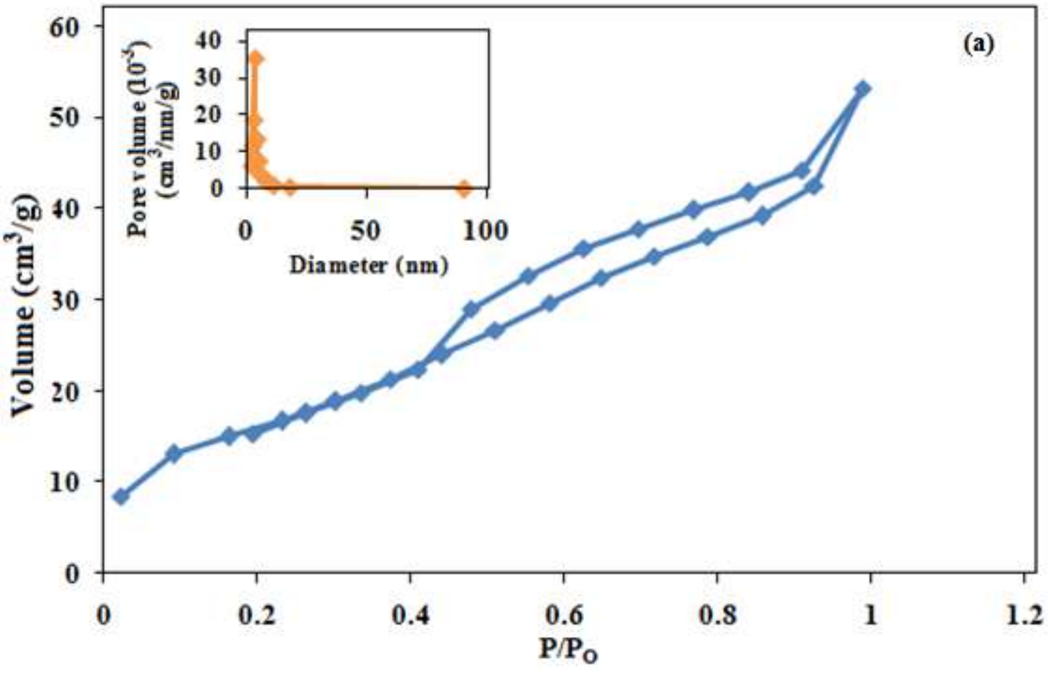

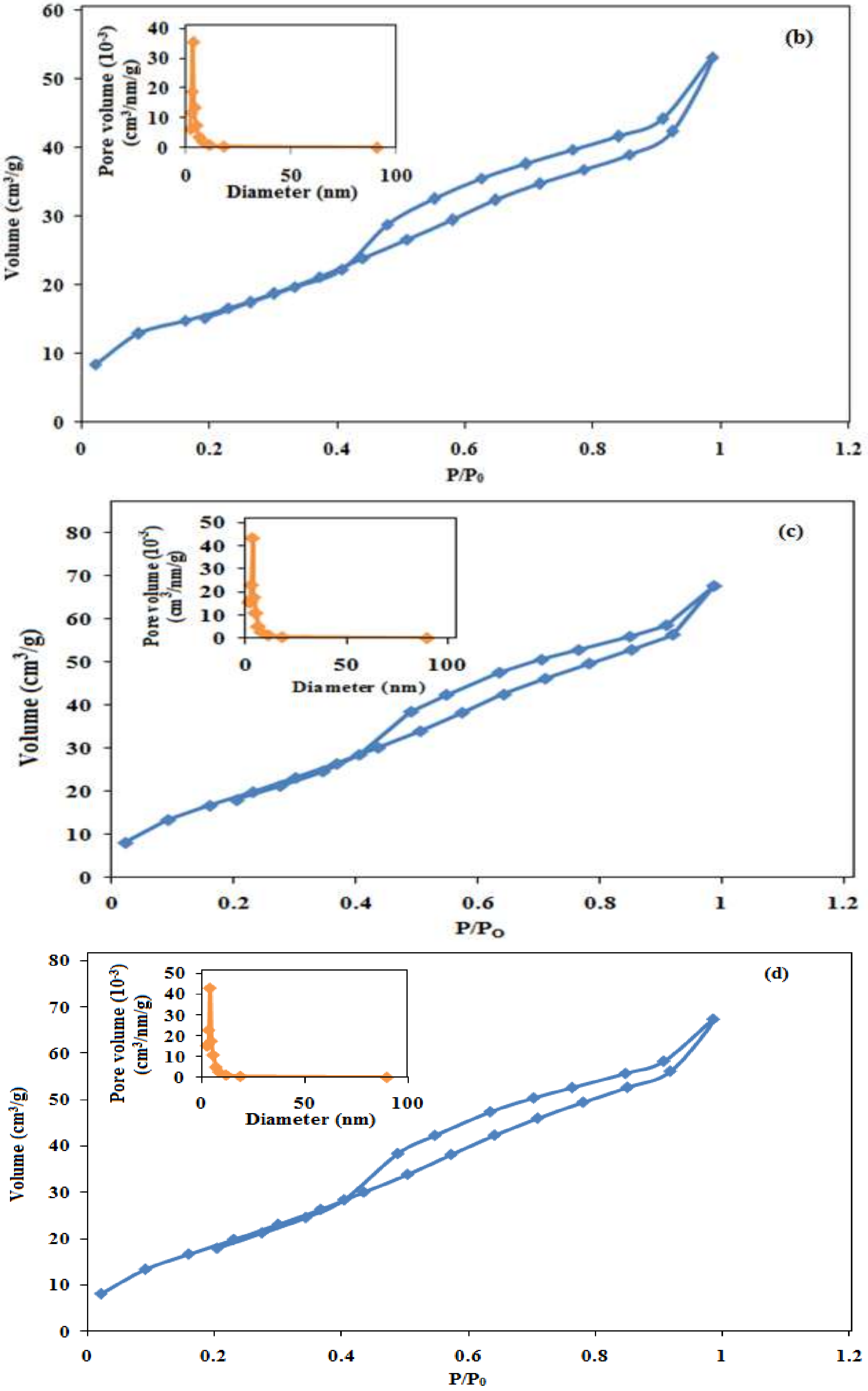

Fig.4.4 N_2 adsorption isotherms and corresponding pore size distribution (inset)

(a) E-1 (b) E-2 (c) E- 3 (d) E-4

4.6 Magnetic Studies

The ferrimagnetic nature of NPs was revealed by s-shaped hysteresis loop as shown in Fig. 4.5. The value of M_s, M_r, and H_c were 7.8, 4.33 emug^{-1} and 415.7 respectively. The modification in magnetic character of the synthesized NPs on coating with CTAB was also evident from the loop and the magnetic parameters of the prepared NPs set out in Table 4.3. Narrow loop denoted low coercively values which showed that the samples can be demagnetized easily (Huang *et al* 2006). The as synthesized surfactant coated NPs showed a decreased value of M_S due to presence of CTAB which is nonmagnetic in nature.

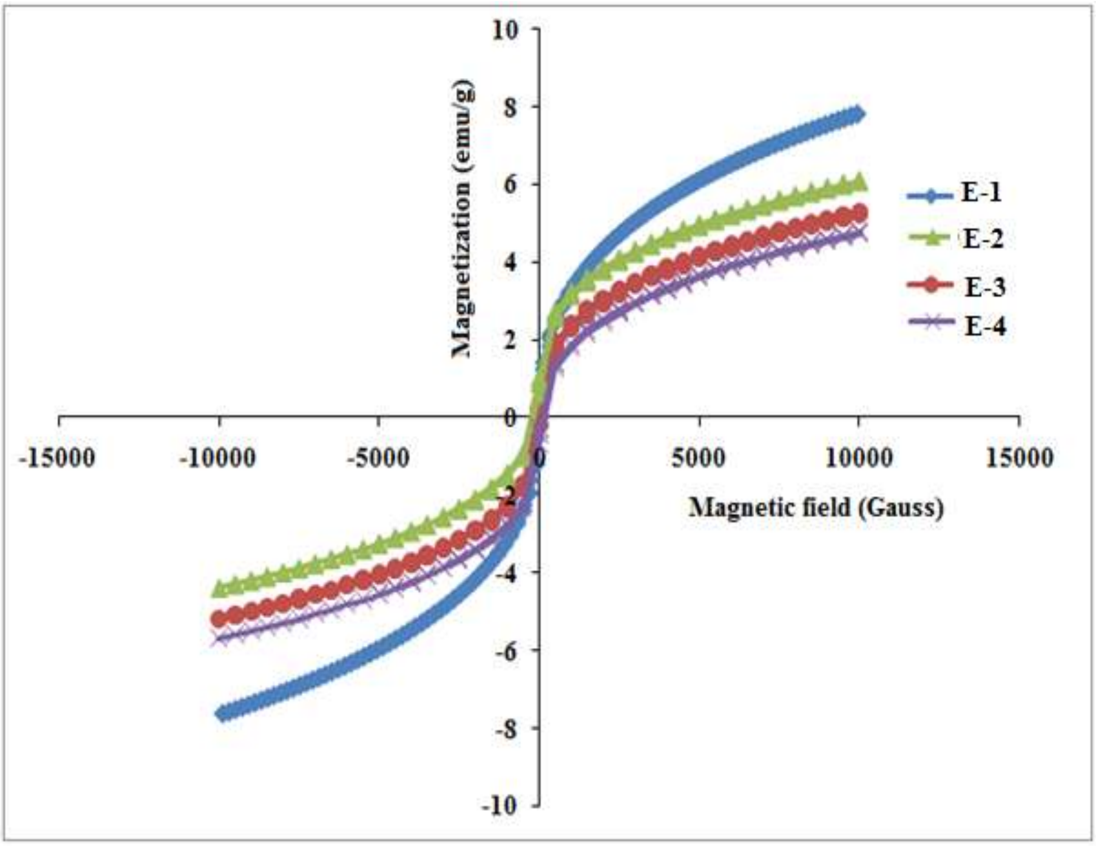

Fig. 4.5: Hysteresis loops of synthesized NPs

Table 4.3 Saturation magnetization, retentivity and coercivity of as synthesized NPs

NPs	Saturation magnetization (M_s) (emu g^{-1})	Retentivity (emu g^{-1})	Coercivity (H_c) (O_e)
E-1	7.8	4.3	415.7
E-2	6.3	1.7	276.6
E-3	5.1	0.9	92.2
E-4	4.3	0.5	76.8

4.7 Enzymatic studies

4.7.1 Mechanism of peroxidase like activity of synthesized NP

In the presence of H_2O_2, the peroxidase like activity of synthesized NPs was investigated by using o-dianisidine dihydrochloride as substrate. Chromogenic substrate o-dianisidine dihydrochloride possesses charge character opposite to that of synthesized NPs as indicated by their zeta potentials (Zhang 2018), which enhances its ability to interact with NPs. Bare and CTAB coated $MgFe_2O_4$ NPs could catalyze the oxidation of o–dianisidine dihydrochloride using H_2O_2 producing a dark brown colored solution. As shown in Fig. 4.7 the color of the CTAB@$MgFe_2O_4$NPs-H_2O_2-substrate system showed increased absorbance than CTAB@$MgFe_2O_4$ NPs- substrate system whereas no color was produced by H_2O_2-substrate system. It indicates that in the presence of H_2O_2, CTAB@$MgFe_2O_4$ NPs possess peroxidase like activity. The expected reaction mechanism for the peroxidase-like activity of NPs is shown in Fig. 4.6. These NPs catalyzed the decomposition of H_2O_2 to produce hydroxyl radicals, which produced dark brown solution (oxidized product) on oxidation of o-dianisidine dihydrochloride.

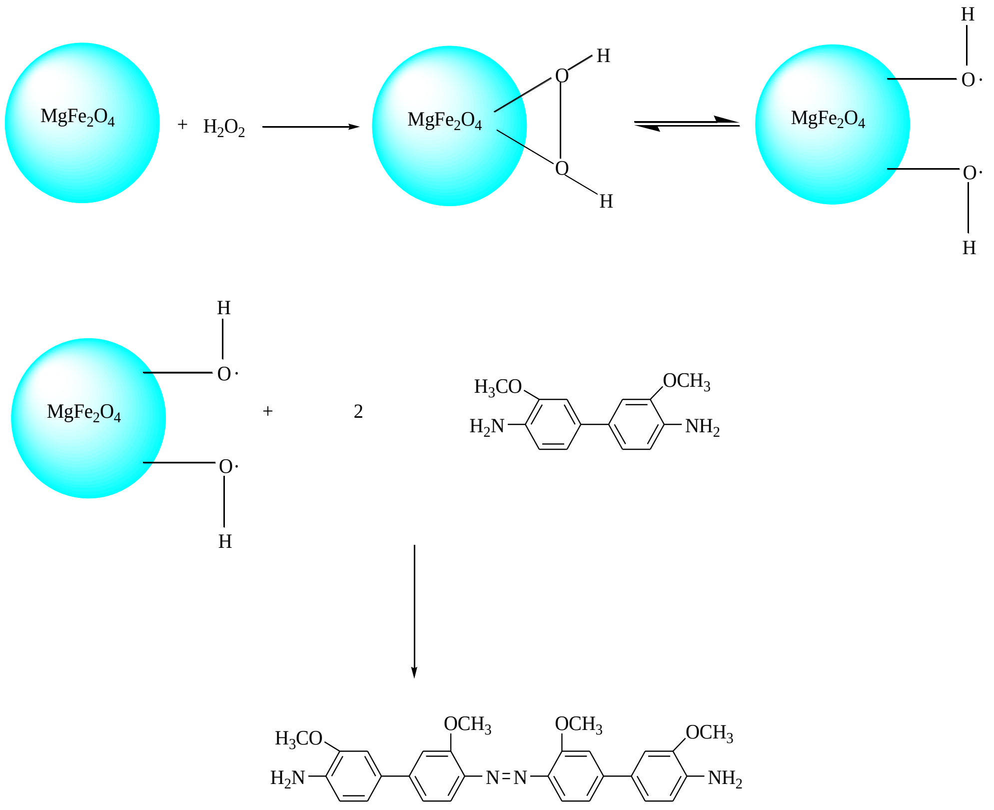

Fig. 4.6: Mechanism of peroxidase mimic activity of $MgFe_2O_4$ NPs

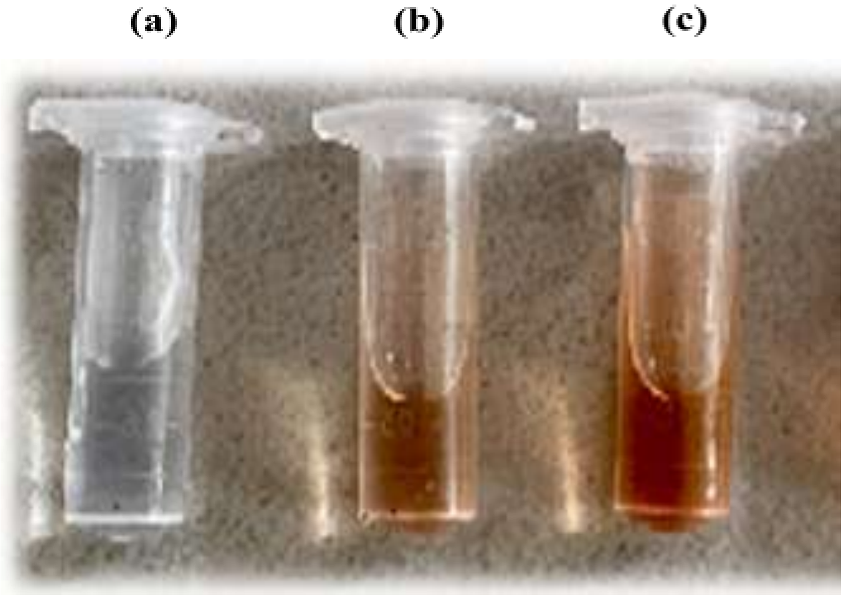

Fig. 4.7: (a) Substrate-H_2O_2 system (b) CTAB@$MgFe_2O_4$NPs-substrate system (c)CTAB@$MgFe_2O_4$NPs-H_2O_2-substrate system

4.7.2 Effect of pH

The effect of pH played a pivotal role in altering the peroxidase activity of CTAB@$MgFe_2O_4$NPs. For observing the peroxidase like activity of NPs, the pH of the reaction mixture was varied from 1.0-9.0 (Table 4.4 and Fig. 4.8) at 25°C. The highest activity of the synthesized NPs was observed at pH 1.0, which further decreased on increasing pH of the reaction mixture. For peroxidase mimic, under acidic medium, the H^+ ions attack on lone pair of oxygen atom thus, weaken O-O bond in H_2O_2 that results in its rapid breakdown, thus increases the rate of reaction.

Table 4.4: Statistical data expressed as mean ± standard deviation for effect of pH on peroxidase activity

pH	**Nanozyme**
	$MgFe_2O_4$
1.0	0.21±0.005
3.0	0.19±0.008
5.0	0.13±0.009
7.0	0.05±0.007
9.0	0.03±0.004

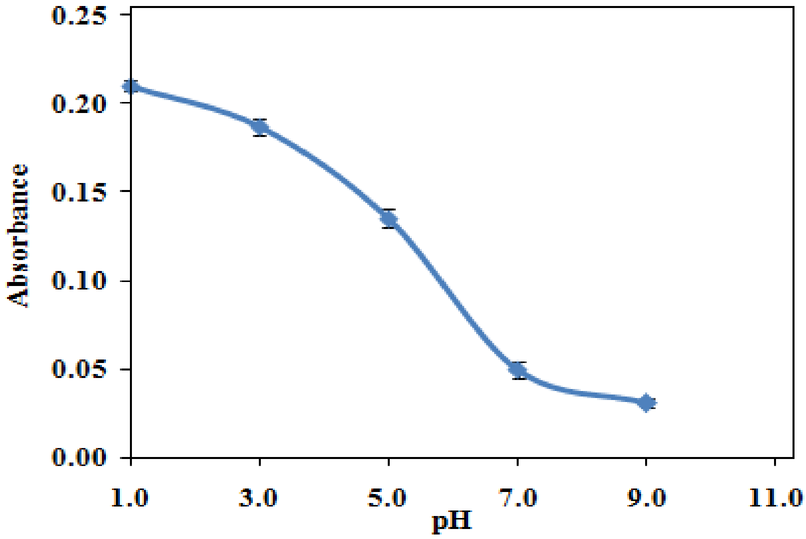

Fig. 4.8: Effect of pH on absorbance of solution in the presence of E-3 NPs

4.7.3 Comparison of peroxidase like activity of synthesized NPs

Peroxidase mimic activity of as synthesized NPs was compared and is shown in Table 4.5 and Fig. 4.9. Surfactant coated NPs displayed greater actiivity than pristine NPs. Due to coating; surface area of $MgFe_2O_4$ NPs increased which results in greater interaction with substrate resulting in enhanced enzyme mimic activity. Among the surfactant coated NPs, maximum activity was exhibited by E-3 followed by E-4, and E-2. These findings indicated that at a lower CTAB concentration, the activity increased as a result of lesser agglomeration of NPs, whereas, at a higher CTAB concentration, the mimic activity decreased due to steric hindrance offered by CTAB to the substrate molecules.

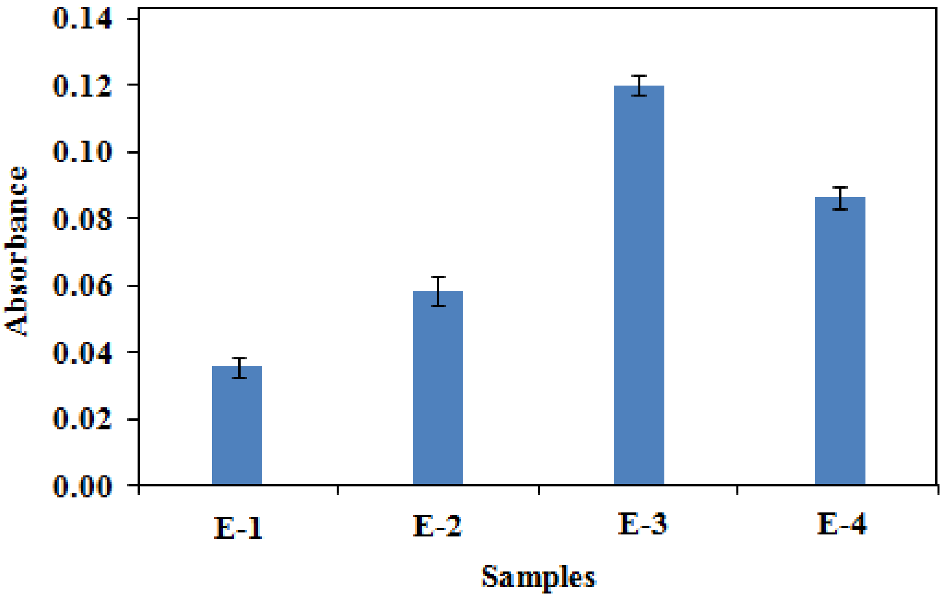

Fig. 4.9: Comparison of activity of different samples

Table 4.5: Statistical data expressed as mean ± standard deviation

Nanozyme	Absorbance
E-1	0.04 ± 0.005^{d}
E-2	0.06 ± 0.008^{c}
E-3	0.12 ± 0.005^{a}
E-4	0.09 ± 0.007^{b}

All the experiments were performed in triplicates and expressed as mean ± Standard deviation in Table 4.5. Superscripts of mean valued were different showed that compounds are significantly different by using ne way ANOVA at p=0.05

4.7.4 Effect of various parameters on peroxidase mimic activity

E-3 NPs showed the best activity among all the synthesized samples. Hence, all the reaction conditions were optimized using this sample.

4.7.4.1 Effect of temperature

The temperature variation from 15º C to 45º C resulted in rise in the rate of reaction up to 25ºC, with further temperature elevation, the reaction rate showed a declining trend signifying that 25°C was the optimum temperature for peroxidase mimic activity of NPs. The drop in activity after optimum temperature was due to the bond breakage between CTAB and $MgFe_2O_4$ NPs due to which the interaction between NPs and substrate decreased (Fig. 4.10 and Table 4.6).

4.7.4.2 Effect of contact time

Effect of contact time on peroxidase like activity was carried out by noting the absorbance at 2 min intervals for 20 min. The optimum contact time was found to be 10 min. Activity of NPs increased with increase in time of contact because more and more NPs interact with substrate as the time increased and hence the absorbance increased as shown in Table 4.7 and Fig. 4.11. Curve flattened after reaching its peak at 10 min, and no more increase is observed after this point.

4.7.4.3 Effect of substrate and NPs dose

Optimization of concentration of substrate and NPs was achieved by varying their content during reaction. Optimum substrate concentration was found to be 2mM (Table 4.8 and Fig. 4.12) and for CTAB@$MgFe_2O_4$ NPs was 5 mg (Table 4.9 and Fig.4.13). Increase in the concentration of NPs till 5 mg increased the absorbance of the oxidized product and afterward it decreased because as the conentration of NPs increased from the optimized limit then NPs started to aggregate and formed clusters and thus resulted in their lower activity.

Table 4.6: Statistical data expressed as mean ± Standard Deviation for effect of temperature on peroxidase activity

Temperature (°C)	Nanozyme
	CTAB@$MgFe_2O_4$ (E-3)
15	0.164±0.001
25	0.175±0.001
35	0.153±0.002
45	0.144±0.001

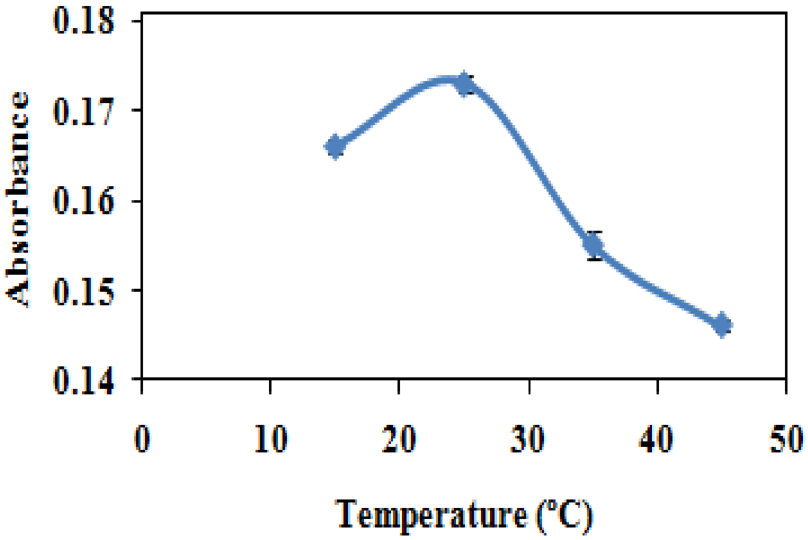

Fig. 4.10: Effect of temperature on absorbance of solution.

Table 4.7: Statistical data expressed as mean ± Standard Deviation for effect of contact time on peroxidase activity

Contact time (min)	Nanozyme
	CTAB@$MgFe_2O_4$ (E-3)
2	0.04±0.006
4	0.08±0.008
6	0.13±0.007
8	0.17±0.009
10	0.21±0.007
12	0.21±0.008
14	0.21±0.009
16	0.21±0.008
18	0.21±0.008
20	0.21±0.009
22	0.21±0.009

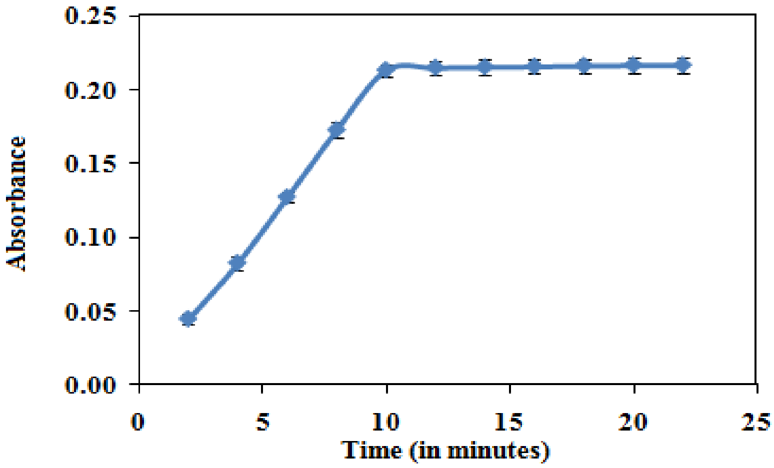

Fig. 4.11: Effect of time on absorbance of solution

Table 4.8: Statistical data expressed as mean ± Standard Deviation for effect of substrate dose on peroxidase activity

Substrate (mM)	Nanozyme
	CTAB@MgFe$_2$O$_4$ (E-3)
1	0.17±0.014
2	0.34±0.011
3	0.31±0.009
4	0.29±0.009
5	0.21±0.006
6	0.18±0.006

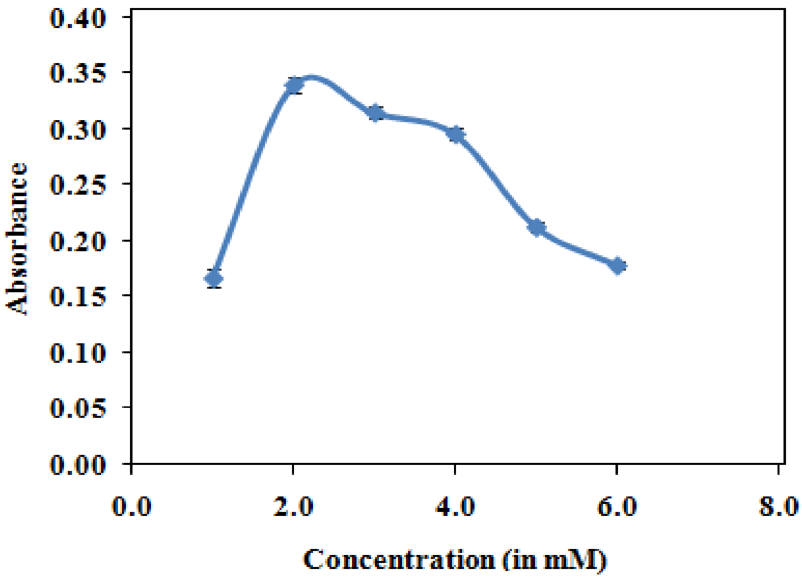

Fig 4.12: Effect of substrate concentration on the absorbance

Table 4.9: Statistical data expressed as mean ± Standard Deviation for effect of catalyst dose on peroxidase mimic activity

Catalyst dose (mg)	Nanozyme
	CTAB@$MgFe_2O_4$ (E-3)
1	0.06±0.004
2	0.07±0.005
3	0.15±0.004
4	0.23±0.007
5	0.29±0.008
6	0.27±0.009

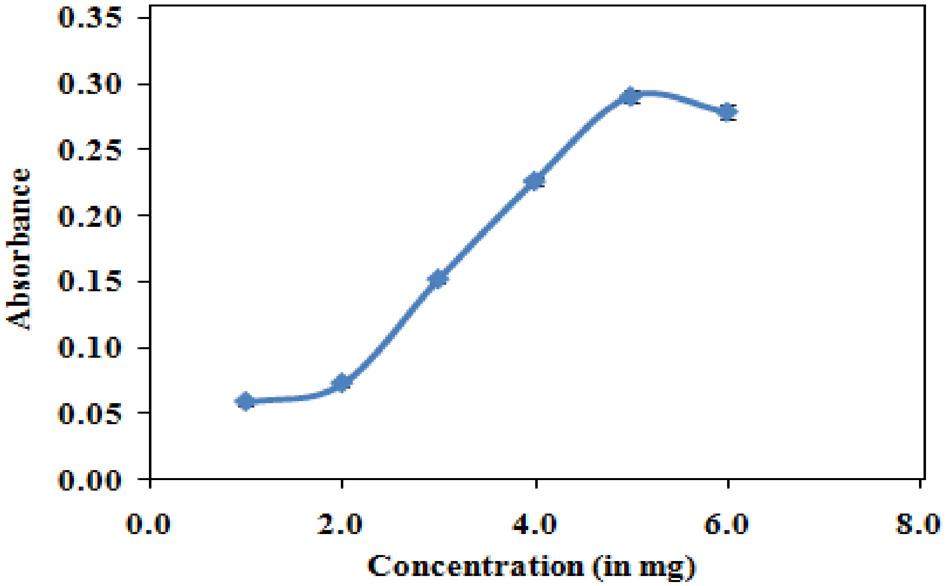

Fig. 4.13: Effect of CTAB@$MgFe_2O_4$ NPs concentration on the absorbance

4.7.5 Kinetic studies of peroxidase like activity

The change in the absorbance of the reaction mixture at 435 nm was noted for 10 min at 2 min intervals for various concentrations of o-dianisidine dihydrochloride. Fig. 4.14 shows the change in absorbance of substrate at different concentration for CTAB@$MgFe_2O_4$ (E-3). The rate constants were determined from log [A_o/ (A_o-A_t)] for different concentrations where A_t and A_o are the absorbance values at a time 't' and at an infinite time respectively. From Fig. 4.15 (a) it was noticed that reaction followed first-order kinetics at low substrate concentrations and zero order at higher substrate concentrations. The kinetic parameters K_m and V_{max} were calculated from the Lineweaver-Burk plot in Fig. 4.15 (b). *K*m and *V* max for different peroxidase mimics is illustrated in Table 4.10.

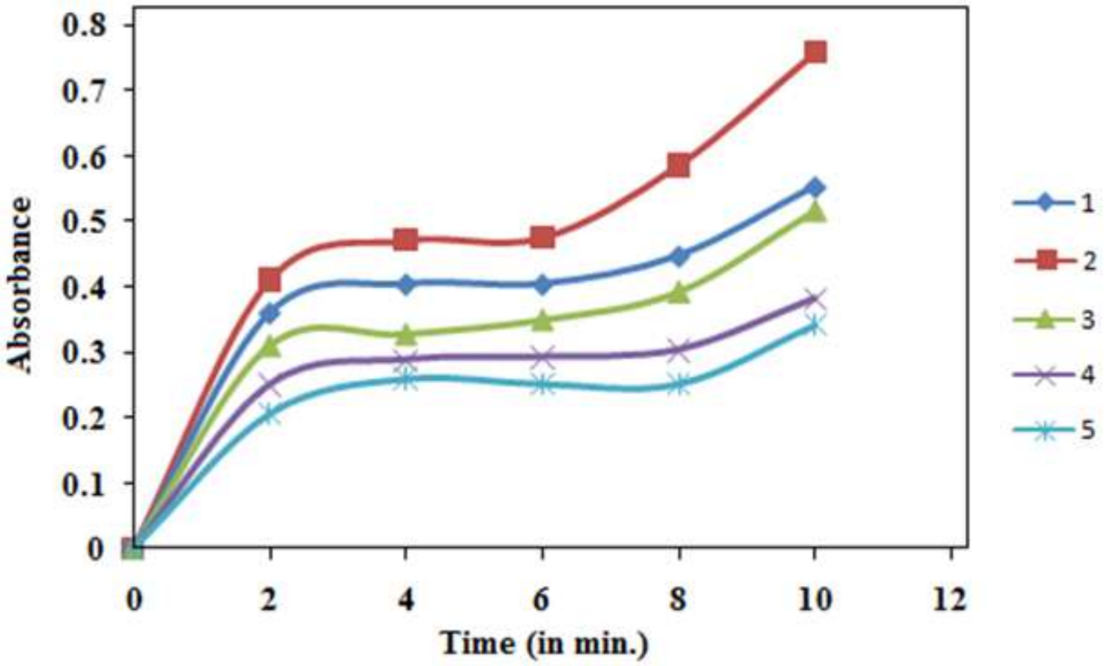

Fig. 4.14: Plot of change in absorbance at 435 nm versus time for various concentrations of o-dianisidine dihydrochloride using E-3 NPs.

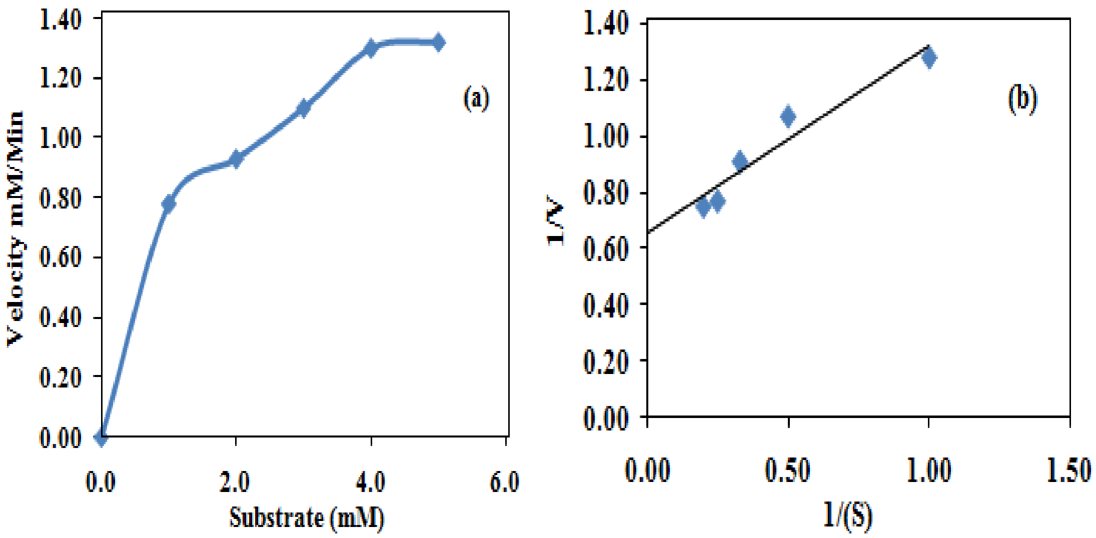

Fig. 4.15: (a) Plot of initial rates versus substrate concentration of oxidation of o-dianisidine dihydrochloride catalysed by E-3 NPs;(b) The Line weaver-Burk plot for E-3 NPs.

Table 4.10: Comparison of K_m and V_{max} between CTAB@$MgFe_2O_4$ and other catalysts

Enzyme	K_m (mM)	V_{max} (mol sec^{-1})	Substrate	Reference
CTAB@Fe_2O_3	7.69	1.12	o-dianisidine dihydrochloride	Garg *et al* 2018
$NiFe_2O_4$	0.55	4.57×10^{-8}	TMB	Su *et al* 2015
	0.46	17.48×10^{-8}	ABTS	
MoS_2@$MgFe_2O_4$	0.81	14.13×10^{-7}	TMB	Zhang *et al* 2018
	1.03	1.41×10^{-8}	ABTS	
HRP	0.43	10×10^{-8}	TMB	Gao *et al* 2007
CTAB@$MgFe_2O_4$	1.01	2.55×10^{-8}	o-dianisidine dihydrochloride	Present work

K_m is an indicator of the enzyme affinity to the substrate. Lower the K_m, stronger is the affinity.

4.8 Detection of H_2O_2 and glucose using CTAB@$MgFe_2O_4$ (1:1) as peroxidase mimics

4.8.1 Detection of H_2O_2

Based on the above results, a sensitive and simple method for the determination of H_2O_2 and glucose was established. As shown in Fig. 4.16, with the increase in concentration of H_2O_2, the absorption spectra of the system of substrate-H_2O_2-catalyst (435 nm) also increased. Fig. 4.17, illustrates the relationship between the absorption intensity of the system and the concentration of H_2O_2 and showed that both are proportional to each other in the range of 20-300 µM (R^2=0.988) with a detection limit of 10 µM.

4.8.2 Detection of glucose

Fig. 4.18 represents the absorption spectra of the system Glucose-GOx-catalyst-substrate at 435 nm increased with the concentration of glucose. Fig.4.19 illustrates the relationship between the glucose concentration and absorption intensity of the system and indicated that both are proportional to each other in the linear range of 10-1000 µM (R^2= 0.97) with a detection limit of 5 µM. The performance of similar peroxidase mimic NPs for detection of hydrogen peroxide and glucose is summarized in Table 4.11. It is clear from the table; the CTAB@$MgFe_2O_4$ had a broad range for detection of glucose as compared to other nanozymes. For H_2O_2, the detection limit is similar to other peroxidase mimics.

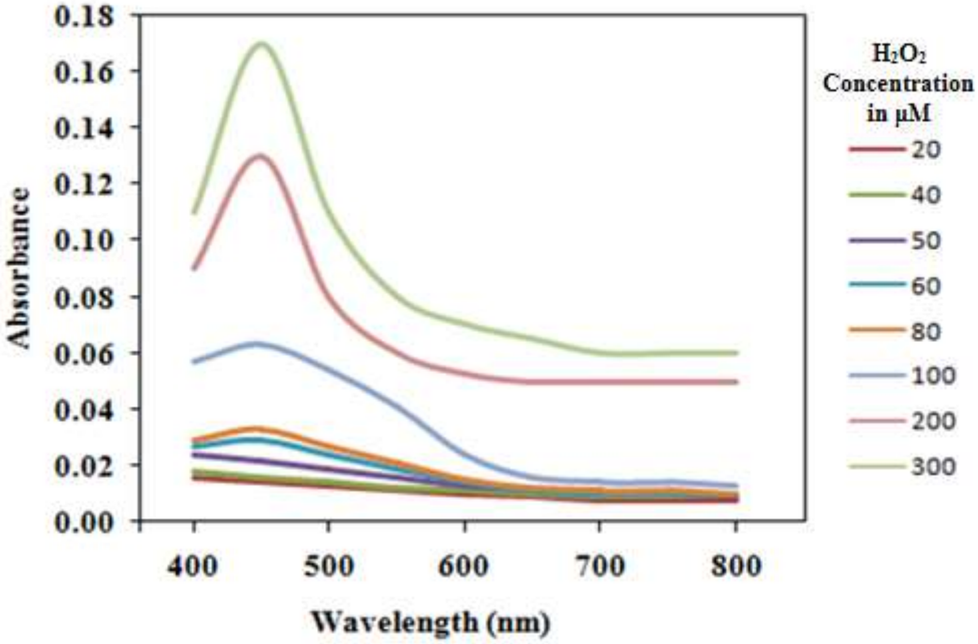

Fig.4.16: The UV-vis absorbance spectrae changes in the presence of H_2O_2

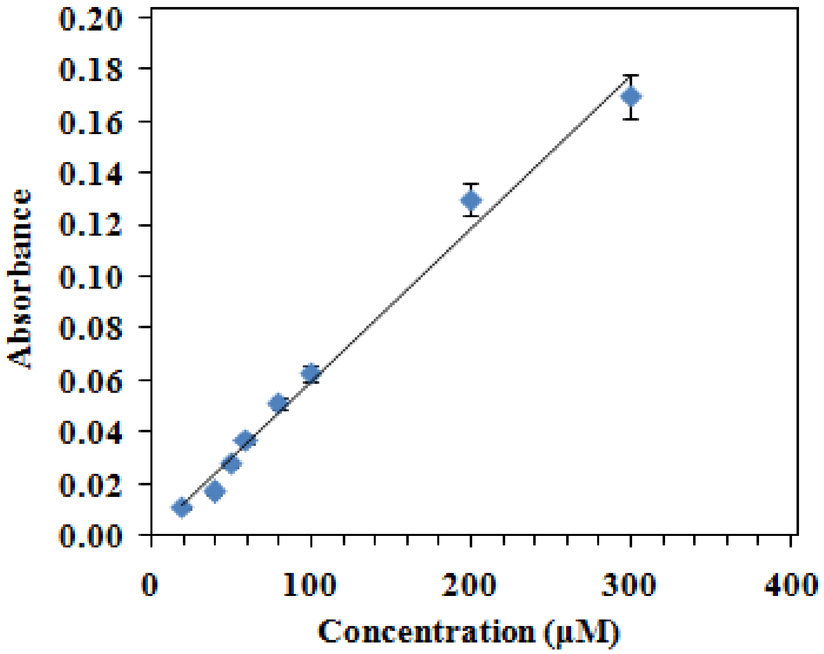

Fig.4.17: The linear calibration plots for H_2O_2detection

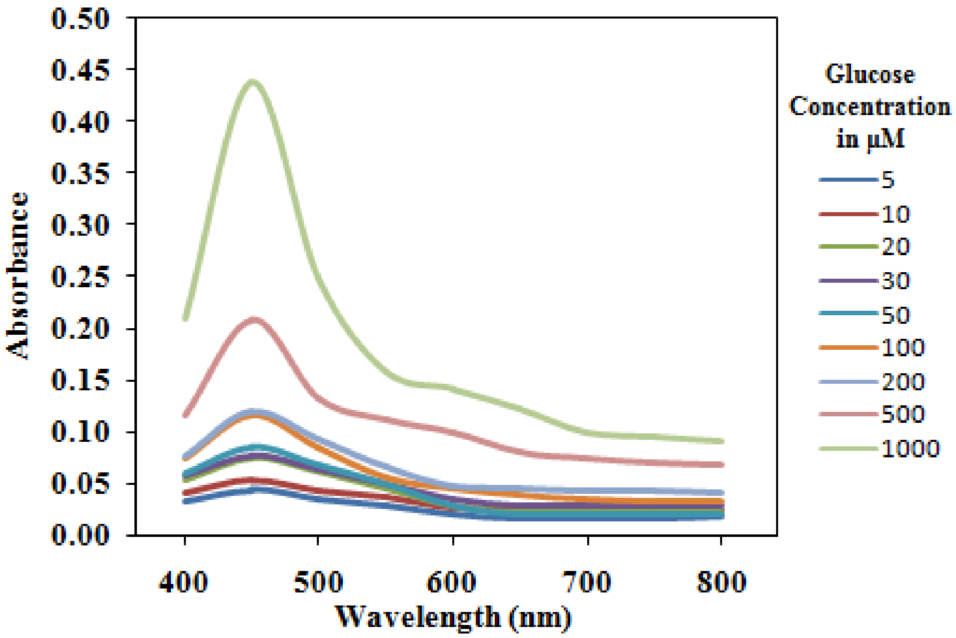

Fig.4.18: The UV-vis absorbance spectra changes in the presence of Glucose

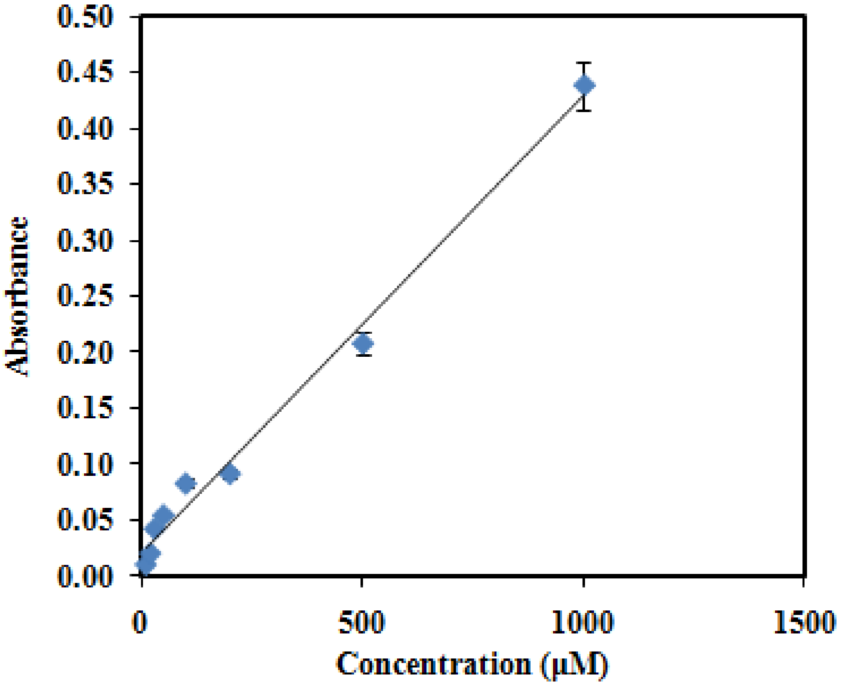

Fig.4.19: The linear calibration plots for glucose detection

Table 4.11: Range and limit of detection of H_2O_2 and Glucose by different peroxidase mimics

Catalyst	Linear range		Limit of Detection		Reference
	H_2O_2 (µM)	Glucose (µM)	H_2O_2 (µM)	Glucose (µM)	
MoS_2 nanosheets	5-100	5-150	1.5	1.2	Lin *et al 2014*
MoS_2@$MgFe_2O_4$	2.5-300	5.0-200	1.0	2.0	Zhang *et al* 2018
$NiFe_2O_4$	-	0.94-25	-	0.45	Su *et al* 2015
Co_3O_4	50-1000	10-1000	10	5	Mu *et al* 2012
$ZnFe_2O_4$@ZnO	-	1-23	-	0.4	Zhao *et al* 2013
SDS-MoS_2	2-100	5-500	0.32	0.57	Zhao *et al* 2015
$ZnFe_2O_4$	-	1.25-18.75	-	0.3	Su *et al* 2012
CTAB@$MgFe_2O_4$	20-300	10-1000	10	5	This work

The stability of CTAB@$MgFe_2O_4$ system stored at room temperature was also examined after 7 days, and similar value of absorbance was observed. Furthermore, the selectivity of this system can be investigated and procedure for biological samples can be standardized.

CHAPTER V

SUMMARY

Natural enzymes have been studied widely since several years due to their high efficiency and specificity towards substrate. But owing to their several drawbacks including rapid digestion by proteases, denaturation on changing environmental conditions and inhibition of their catalytic activity the need for some artificial enzymes was felt due to which enzyme mimicking came as a way out for this shortcoming. Enzymes are the catalysts which fasten the rate of reaction. Artificial enzymes are the synthetic compounds which can exactly imitate the properties of natural ones. Recently, alliance of biology and nanotechnology has ignited the efforts of researchers to develop the functional nanomaterials that can exactly act like enzymes.

NPs are sub micron particles having diameter in the range of 1-100 nm made of organic and inorganic materials. Among the abundant examples of nanomaterial based artificial enzymes, a modern generation of nanomaterials offering high catalytic activity takes one of the most crucial role towards enzyme mimics. Nanocomposites have been anticipated to realize the combined effect of inorganic materials from which nanomaterial is formed that further enhances the activity as compared to its individual precursors. Their properties can be changed by surface modification. A number of low cost and effective NPs have been reported that can exactly mimic the activity of natural enzymes including CoS nanospheres, Co_3O_4 nanowires, $Tb_2(MoO_4)_3$ nanoplates, ZnS nanoribbons, MnO nanopopcorns and many more. Among these, iron oxide (Fe_2O_3) and ferrite nanoparticles (MFe_2O_4NPs) now days are mostly used due to their tremendous properties include electronic, catalytic, biological and chemical properties.

Their size, morphology and surface properties can be changed by altering reaction conditions which further enhances their application potential. By virtue of their high surface to volume ratio, these magnetic NPs possess high surface energy. Present work was related to the synthesis and evaluation of pristine and Cetyl triethyl ammonium bromide (CTAB) coated magnesium ferrite ($MgFe_2O_4$) NPs as peroxidase mimics for detection of H_2O_2 and glucose.

Thesis has been divided into five chapters. First chapter depicts the introduction regarding research problem under examination. Extensive review of literature is contained in the second chapter. Third chapter give the details of the experimental set up, followed by result and discussion (Chapter IV) and summary (chapter V). Pristine $MgFe_2O_4$ NPs were synthesized by sol-gel method and designated as E-1 while, different CTAB concentrations were used to fabricate surfactant coated NPs in w/w ratio (CTAB:$MgFe_2O_4$) of 1:2, 1:1, 2:1 and designated as E-2, E-3, and E-4 respectively. The synthesized NPs were characterized by X-Ray diffraction (XRD), Fourier transmission infrared spectroscopy FT-IR, Transmission

Electron Microscopy (TEM), Brunauer-Emmette-Teller (BET) and Vibrating-sample-magnetometer (VSM) analysis.

While XRD revealed the phase purity of the ferrites and confirmed the spinel structure, FT-IR analysis confirmed the presence of CTAB in the E-2, E-3, E-4 samples. Agglomeration of the ferrite magnetic NPs and their spherical morphology was evaluated using TEM. BET studies showed the increased surface area of E-3 NPs as compared to rest of the samples.

The peroxidase like activity of synthesized NPs with o-dianisidine dihydrochloride as substrate was performed in the presence of H_2O_2 using Shannon *et al* (1966) method. Peroxidase like activity of NPs was observed by varying the pH of the reaction mixture from 1.0-9.0. The synthesized NPs showed highest activity at pH 1.0 and activity decreased on further increasing pH of the reaction mixture. Thus pH 1.0 was found to be the optimum pH for NPs. Experiments showed that E-3 NPs showed maximum peroxidase activity than other NPs in consideration owing to its maximum surface area of $78m^2/g$ as depicted by BET analysis. Thus, further experiments were performed by taking E-3 NPs. Similarly, 25°C, 0.635 mg ml^{-1} and 0.25mg ml^{-1} were the optimum temperature, substrate concentration and NPs concentration of the reaction respectively.

Higher peroxidase mimic activity for the E-3 NPs was due to the coating which increased surface area of NPs and stronger interactions with substrate resulting in increased enzyme mimic activity. From Line-Weaver Burk plot, the calculated K_m and V_{max} value of the E-3 NPs were 1.01 mM and 2.55×10^{-8} mol sec^{-1} respectively which indicate greater affinity towards substrate. E-3 NPs were used to detect H_2O_2 and glucose in the linear range of 20-300 µM and 10-1000 µM respectively, with a detection limit of 10 µM for H_2O_2 and 5 µM for glucose.

Thus, the present work showed the future application of surfactant coated ferrite NPs as enzyme mimics and they may also act as potential candidate in the field of biosensors.

REFERENCES

Antisari M V, Marazzi R and Krsmanovic R (2003) Synthesis of multiwall carbon nanotubes by electric arc discharge in liquid environments. *Carbon* **41(12):** 2393-401

Ashour A H, El-Batal A I, Maksoud M A, El-Sayyad G S, Labib S, Abdeltwab E and El-Okr M M (2018) Antimicrobial activity of metal-substituted cobalt ferrite nanoparticles synthesized by sol–gel technique. *Particuology* **40:** 141-51.

Batista C A S, Larson R G and Kotov N A (2015) Nonadditivity of nanoparticle interactions. *Science* **350:** (6257).

Candeia R A, Souza M A F, Bernardi M I B, Maestrelli S C, Santos I M G, Souza A G and Longo E (2006) $MgFe_2O_4$ pigment obtained at low temperature. *Mater Res Bull* **41(1):** 183-90.

Cao Q, Yu L, Zheng L Q, Li G Z, Ding Y H and Xiao J H (2008) Rheological properties of wormlike micelles in sodium oleate solution induced by sodium ion. *Colloids Surf* **312(1):** 32-38.

Cao X and Wang N (2011) A novel non-enzymatic glucose sensor modified with Fe_2O_3 nanowire arrays. *Analyst* **136**:4241-46.

Chakradhary V K, Ansari A and Akhtar M J (2019) Design, synthesis, and testing of high coercivity cobalt doped nickel ferrite nanoparticles for magnetic applications. *J Magn Magn Mater* **469:** 674-80.

Chen C, Wang Y, Yang Z and Zhang D (2019) Layered double hydroxide derived ultrathin 2D Ni-V mixed metal oxide as a robust peroxidase mimic. *Chem Eng* **369:** 161-69.

Chen L, Sun K, Li P, Fan X, Sun J and Ai S (2013) DNA-enhanced peroxidase-like activity of layered double hydroxide nanosheets and applications in H_2O_2 and glucose sensing. *Nanoscale 5***(22):** 10982-88.

Chen J, Ge J, Zhang L, Li Z, Zhou S and Qu L (2015) PSS-GN nanocomposites as highly-efficient peroxidase mimics and their applications in colorimetric detection of glucose in serum. *RSC Adv* **5(110):** 90400-07.

Chen M, Sun L, Ding Y, Shi Z and Liu Q (2017) N, N′-Di-carboxymethyl perylene diimide functionalized magnetic nanocomposites with enhanced peroxidase-like activity for colorimetric sensing of H_2O_2 and glucose. *New J Chem* **41(13):** 5853-62.

Chen Q, Rondinone A J, Chakoumakos B C and Zhang Z J (1999) Synthesis of superparamagnetic $MgFe_2O_4$ nanoparticles by coprecipitation. *J Magn Magn Mater* **194(1-3):** 1-7.

Chourpa I, Eyrolles L D, Okassa L N, Fouquenet J F, Jonathan S C, Souce M, Marchais H and Dubois P (2005) Molecular composition of iron oxide nanoparticles, precursors for magnetic drug targeting, as characterized by confocal raman microspectroscopy. *Royal Soc Chem Adv* **130**:1395-403.

Cullity B D (1976) Some problems in X-ray stress measurements. *Adv X-ray Anal* **20:** 259-71.

Cullity B D (1978) *Elements of X-ray diffraction*.Pp. 96-99 Addwason Wesley Pub Co, Reading MA.

D'Amato R, Falconieri M, Gagliardi S, Popovici E, Serra E, Terranova G and Borsella E (2013) Synthesis of ceramic nanoparticles by laser pyrolysis: From research to applications. *J Anal Appl Pyrolysis* **104:** 461-69.

Daniel R M, Dines M and Petach H H (1996) The denaturation and dehydration of stable enzyme at high temperatures. *Biochem J* **317:**1-11.

Dong J, Lina Song, Jun-Jie Yin, Weiwei He, Yihang Wu, Ning Gu and Yu Zhang (2014) Co_3O_4 nanoparticles with multi-enzyme activities and their application in immunohistochemical assay. *ACS Appl Mater Interfaces* **63**: 1959-70.

Fan D Q, Shang C S, Gu W L, Wang E K and Dong S J (2017) Introducing ratiometric fluorescence to MnO_2 nanosheet-based biosensing: A simple, label-free ratiometric fluorescent sensor programmed by cascade logic circuit for ultrasensitive GSH detection. *Appl Mater Int* **9**:25870-77.

Fan K, Cao C, Pan Y, Lu D, Yang D, Feng J and Yan X (2012) Magnetoferritin nanoparticles for targeting and visualizing tumour tissues. *Nat nanotechnol* **7(7):** 459-64.

Fardood S T, Golfar Z and Ramazani A (2017) Novel sol–gel synthesis and characterization of superparamagnetic magnesium ferrite nanoparticles using tragacanth gum as a magnetically separable photocatalyst for degradation of reactive blue 21 dye and kinetic study. *J Mater Sci- Mater El* **28(22):** 17002-08.

Fu Y and Wang X (2011) Magnetically separable $ZnFe_2O_4$–graphene catalyst and its high photocatalytic performance under visible light irradiation. *Ind Eng Chem Res* **50(12):** 7210-18.

Gao L, Zhuang J, Nie L, Zhang J, Zhang Y, Gu N and Yan X (2007) Intrinsic peroxidase-like activity of ferromagnetic nanoparticles. *Nat Nanotechnol* **2(9):** 577-83.

Gao Y, Wang G, Huang H, Hu J, Shah S M and Su X (2011) Fluorometric method for the determination of hydrogen peroxide and glucose with Fe_3O_4 as catalyst. *Talanta* **85(2):** 1075-80.

Garg D, Kaur M, Sharma S and Verma V (2018) Effect of CTAB coating on structural, magnetic and peroxidase mimic activity of ferric oxide nanoparticles. *Bull Mater Sci* **41(5)**: 134.

Haikarainen T, Paturi P, Linden J, Haataja S, Klaucke W M, Finne J and Papageorgiou A C (2011) Magnetic properties and structural characterization of iron oxide nanoparticles formed by *Streptococcus suis* dpr and four mutants. *J Biol Inorg Chem* **16**:799-807.

Hao J, Zhang Z, Yang W, Lu B, Ke X., Zhang B and Tang J (2013) In situ controllable growth of $CoFe_2O_4$ ferrite nanocubes on graphene for colorimetric detection of hydrogen peroxide. *J Mater Chem* **1(13):** 4352-57.

He S, Huang Y, Huang J, Liu W, Yao T, Jiang S and Liu Q (2015).Ultrathin CoOOH oxides nanosheets realizing efficient photocatalytic hydrogen evolution. *J Phys Chem* **119(47):** 26362-66.

He S, Shi W, Zhang X, Li J and Huang Y (2010) β−cyclodextrins-based inclusion complexes of $CoFe_2O_4$ magnetic nanoparticles as catalyst for the luminol chemiluminescence system and their applications in hydrogen peroxide detection. *Talanta* **82(1):** 377-83.

He D, Wang P, Zhao K, Xia Z and Liu T (2017) Method for catalyzing TMB and ABTS by using nano metal oxide as oxidase mimetic. *Anal Chim Acta* **64**:89-95

Hosseini M, Sabet F S, Khabbaz H, Aghazadeh M, Mizani F and Ganjali M R (2017) Enhancement of the peroxidase-like activity of cerium-doped ferrite nanoparticles for colorimetric detection of H_2O_2 and glucose. *Anal* **9(23):** 3519-24.

Hu A L, Liu Y H, Deng H H, Hong G L, Liu A L, Lin X H and Chen W (2014) Fluorescent hydrogen peroxide sensor based on cupric oxide nanoparticles and its application for glucose and l-lactate detection. *Biosens Bioelectron* **61:** 374-78.

Hu J, Galvita V V, Poelman H, Detavernier C and Marin G B (2017) A core-shell structured $Fe_2O_3/ZrO_2@ZrO_2$ nanomaterial with enhanced redox activity and stability for CO_2 conversion. *J CO_2 Util* **17:** 20-31.

Hu L, Yuan Y, Zhang L, Zhao J, Majeed S and Xu G (2013) Copper nanoclusters as peroxidase mimetics and their applications to H_2O_2 and glucose detection. *Anal Chim Acta* **762:** 83-86.

Huang W Y, Du P Y, Weng W J and Han G R (2005) Ni-Zn Ferrites Nanoparticle Prepared Directly Using a Sol Precursor by Self-combustion Technique. *Mat Sci Eng A– Struct* **23(5):** 528.

Huang Y, Tang Y, Wang J and Chen Q (2006) Synthesis of $MgFe_2O_4$ nanocrystallites under mild conditions. *Mater Chem Phys* **97(2-3)**: 394-97.

Hussein S I, Elkady A S, Rashad M M, Mostafa A G and Megahid R M (2015) Structural and magnetic properties of magnesium ferrite nanoparticles prepared via EDTA-based sol–gel reaction. *J Magn Magn Mater* **379:** 9-15.

Ichiyanagi Y, Kubota M, Moritake S, Kanazawa Y, Yamada T and Uehashi T (2007) Magnetic properties of Mg-ferrite nanoparticles. *J Magn Magn Mater* **310(2):** 2378-80.

Jiao X, Song H, Zhao H, Bai W, Zhang L and Lv Y (2012) Well-redispersed ceria nanoparticles: promising peroxidase mimetics for H_2O_2 and glucose detection. *Anal* **4(10):** 3261-67.

Jv Y, Li B and Cao R (2010) Positively-charged gold nanoparticles as peroxidiase mimic and their application in hydrogen peroxide and glucose detection. *Chem Comm* **46(42):** 8017-79.

Kaur M, Kaur N, Jeet K and Kaur P (2015) $MgFe_2O_4$ nanoparticles loaded on activated charcoal for effective removal of Cr (VI)–A novel approach. *Ceram Int* **41(10):** 13739-50.

Kaur M, Rana S and Tarsikka P S (2012) Comparative analysis of cadmium doped magnesium ferrite $Mg_{(1-x)}Cd_xFe_2O_4$ (x= 0.0, 0.2, 0.4, 0.6) nanoparticles. *Ceram Int* **38(5):** 4319-23.

Kaur M, Singh M, Mukhopadhyay S S, Singh D and Gupta M (2015) Structural, magnetic and adsorptive properties of clay ferrite nanocomposite and its use for effective removal of Cr (VI) from water. *J Alloys Compd* **653:** 202-11.

Kaur N and Kaur M (2014) Comparative studies on impact of synthesis methods on structural and magnetic properties of magnesium ferrite nanoparticles. *Process Appl Ceram* **8(3)**: 137-43.

Kim M I, Shim J, Li T, Lee J and Park H G (2011) Fabrication of nanoporous nanocomposites entrapping Fe_3O_4 magnetic nanoparticles and oxidases for colorimetric biosensing. *Chem Eur J* **17(38):** 10700-07.

Komarneni S and Katsuki H (2010) Microwave-hydrothermal synthesis of barium titanate under stirring condition. *Ceram Int* **36(3):** 1165-69.

Kuppayee M, Nachiyar G V and Ramasamy V (2012) Enhanced photoluminescence properties of ZnS: Cu^{2+} nanoparticles using PMMA and CTAB surfactants. *Mater Sci Semicond Process* **15(2)**: 136-44.

Lassoued A, Lassoued M S, Dkhil B, Ammar S and Gadri A (2018) Synthesis, photoluminescence and Magnetic properties of iron oxide (α-Fe_2O_3) nanoparticles through precipitation or hydrothermal methods. *Physica E Low Dimens* **101:** 212-19.

Lau I P, Chen H, Wang J, Ong H C, Leung K C F, Ho H P and Kong S K (2012) In vitro effect of CTAB-and PEG-coated gold nanorods on the induction of eryptosis/erythroptosis in human erythrocytes. *Nanotoxicology* **6(8):** 847-56.

Li J, Liu W, Wu X and Gao X (2015) Mechanism of pH-switchable peroxidase and catalase-like activities of gold, silver, platinum and palladium. *Biomaterials* **48**: 37-44

Lin T, Zhong L, Guo L, Fu F, and Chen G (2014) Seeing diabetes: visual detection of glucose based on the intrinsic peroxidase-like activity of MoS_2 nanosheets. *Nanoscale* **6(20)**: 11856-62.

Liu B, Sun Z, Huang P J J and Liu J (2015) Hydrogen peroxide displacing DNA from nanoceria: mechanism and detection of glucose in serum. *J Am Chem Soc* **137(3):** 1290-95.

Liu C P, Li M W, Cui Z, Huang J R, Tian Y L, Lin T and Mi W B (2007) Comparative study of magnesium ferrite nanocrystallites prepared by sol–gel and coprecipitation methods. *J Mater Sci* **42(15):** 6133-38.

Liu F, He J, Zeng M, Hao J, Guo Q, Song Y and Wang L (2016) Cu–hemin metal-organic frameworks with peroxidase-like activity as peroxidase mimics for colorimetric sensing of glucose. *J Nanopart Res* **18(5):** 1-9.

Liu Y L, Liu Z M, Yang Y, Yang H F, Shen G L and Yu R Q (2005) Simple synthesis of $MgFe_2O_4$ nanoparticles as gas sensing materials. *Sens Actuators B Chem* **107(2):** 600-04

Liu Y, Yuan M, Qiao L and Guo R (2014) An efficient colorimetric biosensor for glucose based on peroxidase-like protein-Fe_3O_4 and glucose oxidase nanocomposites. *Biosens Bioelectron* **52:** 391-96.

Long M, Jiang J, Li Y, Cao R, Zhang L and Cai W (2011) Effect of gold nanoparticles on the photocatalytic and photoelectrochemical performance of Au modified $BiVO_4$. *Nano-Micro Lett* **3(3):** 171-77.

Lou Z, He M, Wang R, Qin W, Zhao D and Chen C (2014) Large-scale synthesis of monodisperse magnesium ferrite via an environmentally friendly molten salt route. *Inorg Chem* **53(4):** 2053-57.

Lu Y, Yu J, Ye W, Yao X, Zhou P, Zhang H and Jia, L (2016) Spectrophotometric determination of mercury (II) ions based on their stimulation effect on the peroxidase-like activity of molybdenum disulfide nanosheets. *Microchim Acta* **183(8):** 2481-89.

Luo L, Zhang Y, Li F, Si X, Ding Y, Deng D and Wang T (2013) Enzyme mimics of spinel-type CoxNi1− xFe_2O_4 magnetic nanomaterial for eletroctrocatalytic oxidation of hydrogen peroxide. *Anal Chim Acta* **788:** 46-51.

Luo W, Li Y S, Yuan J, Zhu L, Liu Z, Tang H and Liu S (2010) Ultrasensitive fluorometric determination of hydrogen peroxide and glucose by using multiferroic $BiFeO_3$ nanoparticles as a catalyst. *Talanta* **81(3):** 901-07.

Maddinedi S B and Mandal B K (2014) Peroxidase Like Activity of Quinic Acid Stabilized Copper Oxide Nanosheets *J Anal Pharm* **1:** 1008-16.

Maensiri S, Sangmanee M and Wiengmoon A (2009) Magnesium ferrite ($MgFe_2O_4$) nanostructures fabricated by electrospinning. *Nanoscale Res Let* **4(3):** 221.

Maji S K, Dutta A K, Dutta S, Srivastava D N, Paul P, Mondal A and Adhikary B (2012) Single-source precursor approach for the preparation of CdS nanoparticles and their photocatalytic and intrinsic peroxidase like activity. *Appl Catal* **126:** 265-74.

Majidi S, Zeinali Sehrig F, Farkhani S M, Soleymani Goloujeh M, and Akbarzadeh A (2016) Current methods for synthesis of magnetic nanoparticles. *Artif Cell Nanomed B* **44(2):** 722-34.

Mitra K, Ghosh A B, Sarkar A, Saha N and Dutta A K (2014) Colorimetric estimation of human glucose level using γ-Fe_2O_3 nanoparticles: an easily recoverable effective mimic peroxidase. *Biochem Bioph Res Co* **451(1):** 30-35.

Mu J, Wang Y, Zhao M and Zhang L (2012) Intrinsic peroxidase-like activity and catalase-like activity of Co_3O_4 nanoparticles. *Chem Comm* **48(19)**: 2540-42.

Nag P, Banerjee S, Lee Y, Bumajdad A, Lee Y and Devi P S (2012) Sonochemical synthesis and properties of nanoparticles of $FeSbO_4$. *Inorg Chem* **51(2):** 844-50.

Narita A (2019) Bottom-up Chemical Synthesis of Atomically Precise Graphene Nanoribbons and Their Potentials.

Naseri M G, Ara M H M, Saion E B and Shaari A H (2014) Superparamagnetic magnesium ferrite nanoparticles fabricated by a simple, thermal-treatment method. *J Magn Magn Mater* **350:** 141-47.

Natalio F, André R, Hartog A F, Stoll B, Jochum K P, Wever R and Tremel W (2012) Vanadium pentoxide nanoparticles mimic vanadium haloperoxidases and thwart biofilm formation. *Nat Nanotechnol* **7(8):** 530-35.

Navadeepthy D, Rebekah A, Viswanathan C and Ponpandian N (2017) N-doped Graphene/$ZnFe_2O_4$: A novel nanocomposite for intrinsic peroxidase based sensing of H_2O_2. *Mater Res Bull* **95:** 1-8.

Nguyen L T, Nguyen L T, Manh N C, Quoc D N, Quang H N, Nguyen H T and Bach L G (2019) A facile synthesis, characterization, and photocatalytic activity of magnesium ferrite nanoparticles via the solution combustion method. *J Chem2019.*

Niu X, He Y, Pan J, Li X, Qiu F, Yan Y and Lan M (2016) Uncapped nanobranch-based CuS clews used as an efficient peroxidase mimic enable the visual detection of hydrogen peroxide and glucose with fast response. *Analytica Chimica Acta* **947:** 42-49

Offermanns H, Dittrich G and Steiner N (2000) (Hydrogen peroxide in environmental protection and synthesis). *Chemie in Unserer Zeit* **34(3):** 150-59.

Pandey P C, Singh R and Pandey Y (2015) Controlled synthesis of functional Ag, Ag–Au/Au–Ag nanoparticles and their Prussian blue nanocomposites for bioanalytical applications. *RSC Adv* **5(61)**: 49671-79.

Pasquato L, Pengo P and Scrimin P (2005) Nanozymes: Functional nanoparticle-based catalysts. *Supramol Chem* **17(1-2):** 163-71.

Patil J Y, Khandekar M S, Mulla I S and Suryavanshi S S (2012) Combustion synthesis of magnesium ferrite as liquid petroleum gas (LPG) sensor: effect of sintering temperature. *Curr Appl Phys* **12(1):** 319-24.

Petersen M C, Vatner D F and Shulman G I (2017) Regulation of hepatic glucose metabolism in health and disease. *Nat Rev Endocrinol* **13(10):** 572-87.

Pradeep A, Priyadharsini P and Chandrasekaran G (2008) Sol–gel route of synthesis of nanoparticles of $MgFe_2O_4$ and XRD, FTIR and VSM study. *J Magn Magn Mater* **320(21)**: 2774-79.

Pradhan S K, Bid S, Gateshki M and Petkov V (2005) Microstructure characterization and cation distribution of nanocrystalline magnesium ferrite prepared by ball milling. *Mater Chem Phys* **93(1):** 224-30.

Ragg R, Tahir M N and Tremel W (2016) Solids go bio: inorganic nanoparticles as enzyme mimics. *Eur J Inorg* **2016(13-14):** 1906-15.

Randhawa B S, Kaur H, Dosanjh H S and Singh J (2016) Precursor route for the synthesis of $MgFe_2O_4$ nanoparticles from the thermolysis of magnesium hexapropionatoferrate (III). *Ceram Int* **42(7):** 8891-94.

Rashad M M (2007) Magnetic properties of nanocrystalline magnesium ferrite by co-precipitation assisted with ultrasound irradiation. *J Mater Sci* **42(13):** 5248-55.

Ren H, Ma T, Zhao J and Zhou R (2018) Vc-Functionalized Fe3O4 Nanocomposites as Peroxidase-like Mimetics for H_2O_2 and Glucose Sensing. *Chem Res Chin Univ* **34(2):** 260-68.

Salah N, Habib S S, Khan Z H, Memic A, Azam A, Alarfaj E and Al-Hamedi S (2011) High-energy ball milling technique for ZnO nanoparticles as antibacterial material. *Int J Nanomedicine* **6:** 863

Sawai S, Nakahara Y, Matsumoto N, Choi J, Kato T and Kawaguchi M (2014) Synthesis and characterization of carbon nanoparticle films prepared by plasma-based ion implantation. *Surf Interface Anal* **46(10-11):** 961-65.

Šepelák V, Feldhoff A, Heitjans P, Krumeich F, Menzel D, Litterst F J and Becker K D (2006) Nonequilibrium cation distribution, canted spin arrangement, and enhanced magnetization in nanosized $MgFe_2O_4$ prepared by a one-step mechanochemical route. *Chem Mater* **18(13):** 3057-67.

Shannon LM, Kay E, Lew J Y (1966) Peroxidase isozymes from horseradish roots. I. Isolation and physical properties. *J Biol Chem* **241**:2166-72.

Sharma V and Mobin S M (2017) Cytocompatible peroxidase mimic CuO: graphene nanosphere composite as colorimetric dual sensor for hydrogen peroxide and cholesterol with its logic gate implementation. *Sens Actuators B Chem* **240:** 338-48.

Shi W, Wang Q, Long Y, Cheng Z, Chen S, Zheng H and Huang Y (2011) Carbon nanodots as peroxidase mimetics and their applications to glucose detection. *Chem Comm* **47(23):** 6695-97.

Shukla S K, Demir M M, Govender P P, Tiwari A and Shukla S K (2017) Optical fibre based non-enzymatic glucose sensing over Cu^{2+}-doped polyaniline hybrid matrix. *Sens Actuators B Chem* **242:** 522-28.

Singh R P and Venkataraju C (2018) Effect of calcinations on the structural and magnetic properties of magnesium ferrite nanoparticles prepared by sol gel method. *Chin J Phys* **56(5)**: 2218-25.

Spiers H, Parkin I P, Pankhurst Q A, Affleck L, Green M, Caruana D J and Kvick A (2004) Self propagating high temperature synthesis of magnesium zinc ferrites ($Mg_xZn_{(1-x)}$ Fe_2O_3): thermal imaging and time resolved X-ray diffraction experiments. *J Mater Chem* **14(7)**: 1104-11.

Su L, Feng J, Zhou X, Ren C, Li H and Chen X (2012) Colorimetric detection of urine glucose based $ZnFe_2O_4$ magnetic nanoparticles. *Anal chem* **84(13):** 5753-58.

Su L, Qin W, Zhang H, Rahman Z U, Ren C, Ma S and Chen X (2015) The peroxidase/catalase-like activities of MFe_2O_4 (M= Mg, Ni, Cu) MNPs and their application in colorimetric biosensing of glucose. *Biosens Bioelectron* **63:** 384-91.

Taylor R, Al-Mrabeh A and Sattar N (2019) Understanding the mechanisms of reversal of type 2 diabetes. *Lancet Diabetes Endo* **7(9):** 726-36.

Thankachan S, Jacob B P, Xavier S and Mohammed E M (2013) Effect of neodymium substitution on structural and magnetic properties of magnesium ferrite nanoparticles. *Phys Scr* **87(2)**: 025701.

Valko M, Leibfritz D, Moncol J, Cronin M T, Mazur M Telser, J (2007) Free radicals and antioxidants in normal physiological functions and human disease. *Int J Biochem Cell B* **39(1):** 44-84.

Verma S, Potdar H S, Date S K and Joy P A (2004) Synthesis of superparamagnetic magnesium ferrite nanoparticles by microwave-hydrothermal method. *MRS Online Proceedings Library Archive* **818.**

Verma V, Kaur M and Sharma S (2019) Superoxide dismutase mimic activity of spinel ferrite MFe_2O_4 M= Mn, Co and Cu) nanoparticles. *B Mater Sci* **42(3):** 120.

Wang X, Zhao M, Song Y, Liu Q, Zhang Y, Zhuang Y and Chen S (2019) Synthesis of Zn Fe_2O_4/ZnO heterostructures decorated three-dimensional graphene foam as peroxidase mimetics for colorimetric assay of hydroquinone. *Sens Actuators B Chem* **283:** 130-37.

Wu Z, Pu X, Zhu Y, Jing M, Chen Q, Jia X and Ji X (2015) Uniform porous spinel $NiCo_2O_4$ with enhanced electrochemical performances. *J Alloys Compd* **632:** 208-17.

Wu C W, Unnikrishnan B, Tseng Y T, Wei S C, Chang H T and Huang C C (2019) Mesoporous manganese oxide/manganese ferrite nanopopcorns with dual enzyme mimic activities: A cascade reaction for selective detection of ketoses. *J Colloid Interface Sci* **541:** 75-85.

Xiao N, Liu S G, Mo S, Yang Y Z, Han L, Ju Y J and Luo H Q (2018) B, N-carbon dots-based ratiometric fluorescent and colorimetric dual-readout sensor for H_2O_2 and H_2O_2-involved metabolites detection using $ZnFe_2O_4$ magnetic microspheres as peroxidase mimics. *Sens Actuators B Chem* **273:** 1735-43.

Xu Z, Lyu X, Yang B, Cao W, Li R, Zhang X and Liu Q (2019) Meso-tetrakis (4-chlorophenyl) porphyrin functionalized $CuFe_2O_4/SiO_2$ nanocomposites with enhanced peroxidase-like activity conveniently using for visual biosensing at room temperature. *Colloids Surf* **569:** 28-34.

Yang H, Zha J, Zhang P, Xiong Y, Su L and Ye F (2016) Sphere-like CoS with nanostructures as peroxidase mimics for colorimetric determination of H_2O_2 and mercury ions. *RSC Adv* **6(71):** 66963-70.

Yang P, Ding Y, Lin Z, Chen Z, Li Y, Qiang P and Wang Z L (2014) Low-cost high-performance solid-state asymmetric supercapacitors based on MnO_2 nanowires and Fe_2O_3 nanotubes. *Nano Lett* **14(2):** 731-36.

Yang Y, Mao Z, Huang W, Liu L, Li J, Li J and Wu Q (2016) Redox enzyme-mimicking activities of CeO_2 nanostructures: Intrinsic influence of exposed facets. *Scientific Reports* **6:** 35344.

Yang Z, Ma F, Zhu Y, Chen S, Wang C and Lu X (2017) A facile synthesis of $CuFe_2O_4/Cu_9S_8$/PPy ternary nanotubes as peroxidase mimics for the sensitive colorimetric detection of H_2O_2 and dopamine. *Dalton Trans* **46(34):** 11171-79.

Yin Q, Zhang Z, Wu S, Tan J and Meng K (2015) Preparation and characterization of novel cationic–nonionic organo-montmorillonite. *Mater Express* **5(3):** 180-90.

Yu J, Ma D, Mei L, Gao Q, Yin W, Zhang X and Zhao Y (2018) Peroxidase-like activity of MoS_2 nanoflakes with different modifications and their application for H_2O_2 and glucose detection. *J Mater Chem B* **6(3):** 487-98.

Zaidi S A and Shin J H (2016) Recent developments in nanostructure based electrochemical glucose sensors. *Talanta* **149:** 30-42.

Zhang J W, Zhang H T, Du Z Y, Wang X, Yu S H and Jiang H L (2014) Water-stable metal–organic frameworks with intrinsic peroxidase-like catalytic activity as a colorimetric biosensing platform. *Chem Comm* **50(9):** 1092-94.

Zhang Y, Zhou Z, Wen F, Tan J, Peng T, Luo B and Yin S (2018) A flower-like MoS_2-decorated $MgFe_2O_4$ nanocomposite: Mimicking peroxidase and colorimetric detection of H_2O_2 and glucose. *Sens Actuators B Chem* **275**:155-62.

Zhao K, Gu W, Zheng S, Zhang C and Xian Y (2015) SDS–MoS_2 nanoparticles as highly-efficient peroxidase mimetics for colorimetric detection of H_2O_2 and glucose. *Talanta* **14***:* 47-52.

Zhao M, Huang J, Zhou Y, Pan X, He H, Y, Z and Pan X (2013) Controlled synthesis of spinel $ZnFe_2O_4$ decorated ZnO heterostructures as peroxidase mimetics for enhanced colorimetric biosensing. *Chem Comm* **49(69)**: 7656-58.

VITA

Name	**:**	Ekjot Singh
Father's name	**:**	S. Ranjit Singh
Mother's name	**:**	Smt. Parveen Saini
Nationality	**:**	Indian
Date of birth	**:**	19.10.1997
Permanent home address	**:**	H.No. 613/8, Dashmesh Nagar, Tibri Road, Gurdaspur – 143 521, Punjab

EDUCATIONAL QUALIFICATIONS

Master's degree	**:**	Integrated M.Sc. (Hons.) Chemistry
University and year of award	**:**	Punjab Agricultural University, Ludhiana (2020)
OCPA	**:**	7.83/10.00
Title of Master's Thesis	**:**	Hydrogen peroxide and glucose sensing using magnesium ferrite nanoparticles as peroxidase mimics
Awards/Distinctions / Fellowships/ Scholarships	**:**	-